The Abdus Salam International Centre for Theoretical Physics

United Nations Educational, Scientific and Cultural Organization

IAEA
International Atomic Energy Agency

2052-21

Summer College on Plasma Physics

10 - 28 August 2009

The physics of laser-assisted ion acceleration and applications

Vladimir Tikhonchuk

CELIA - Centre Lasers Intenses et Applications
Université Bordeaux 1
France

Summer College on Plasma Physics, Trieste, August 18, 2009

THE PHYSICS OF LASER-ASSISTED ION ACCELERATION AND APPLICATIONS

V. Tikhonchuk

Centre Lasers Intenses et Applications, Université Bordeaux 1, France

Outline

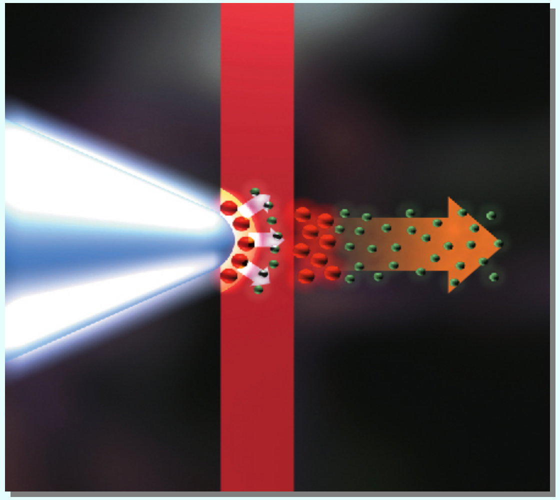

- Motivations
- Ion acceleration under hot electron pressure
  - ion acceleration in the rarefaction wave
  - effect of two electron populations
  - effect of multiple ion species
- Ion acceleration under the radiation pressure
  - laser piston model
  - numerical simulations of ion acceleration
  - effect of radiation losses on the ion acceleration
  - laser acceleration of ultra thin films
- Applications of laser accelerated ions

Ion acceleration with high intensity laser pulses

Fast ions can find many applications in basic science, inertial fusion, industry and medicine. They demonstrate very attractive properties:

- **short acceleration distance (a few μm)**
- **high beam charge (μC)**
- **good laminarity and low emittance**
- **low ratio current/energy flux**
- **simple ballistic transport**
- **high absorption efficiency (Bragg peak)**

$$\varepsilon_{\mathrm{i}} \simeq 45\left(\rho l \,/\, \mathrm{g/cm}^2\right)^{0.56} \mathrm{MeV}$$

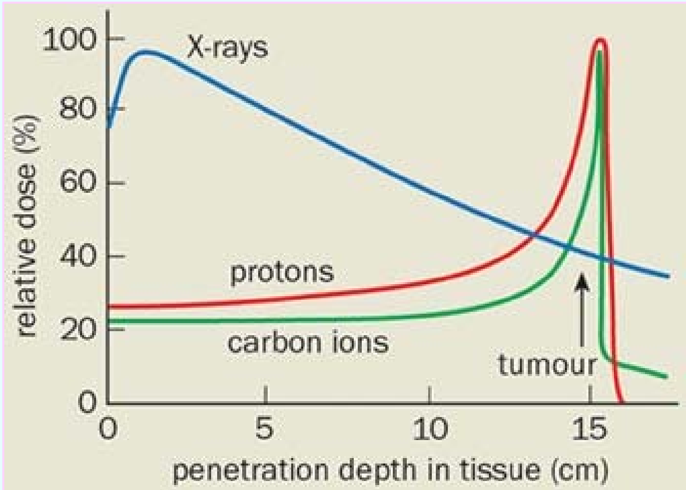

Mechanisms of ion acceleration

Two mechanisms of laser ion acceleration have been considered:

TNSA – target normal sheath acceleration from a narrow layer at the rear side of the target. It requires:

- efficient production of high energy electrons (> 30%)
- high quality target surface
- mild restrictions on the laser pulse (prepulse)
- limited number of ions (< μC)

RPA – radiation pressure acceleration at the front side and in the volume of target. It requires:

- cold electrons (circ polarization)
- high quality laser pulse (very high contrast > 10^{12})
- higher intensities (> 10^{21} W/cm^2)
- mild restrictions on the target
- could be more efficient
- more ions could be accelerated

TNSA mechanism of ion acceleration

Target normal sheath acceleration from a narrow layer at the rear side of the target

- efficient production of high energy electrons (> 30%)
- high quality target surface
- mild restrictions on the laser pulse (prepulse)
- limited number of ions (< µC)

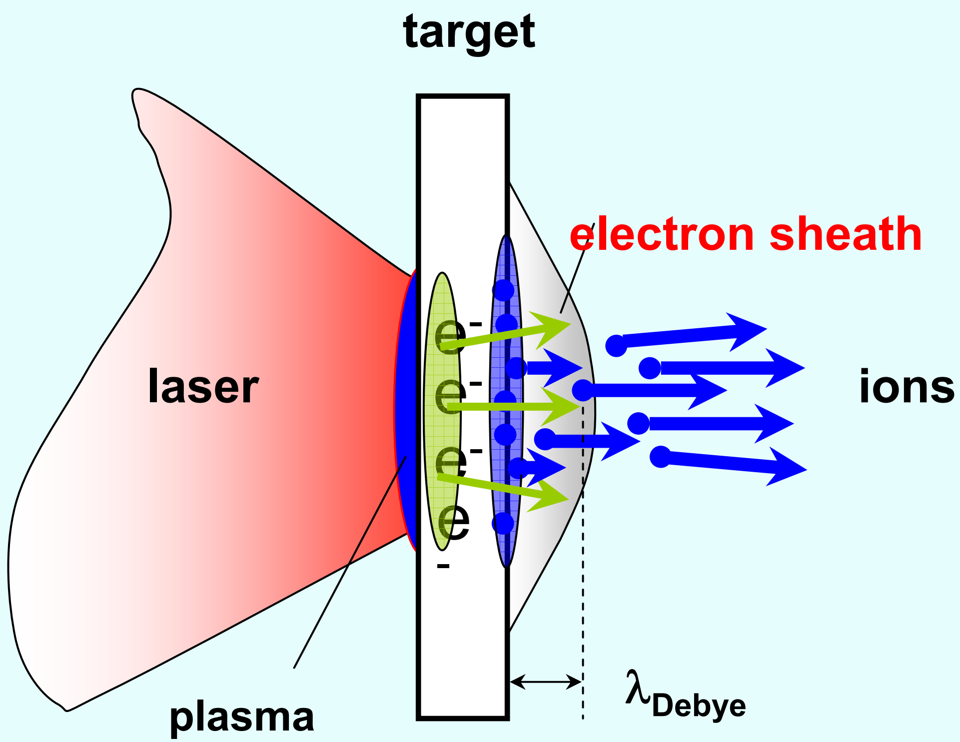

Ion emission from the front side of the target

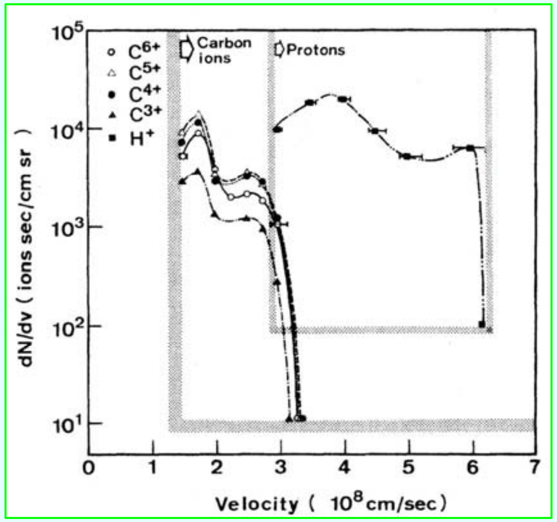

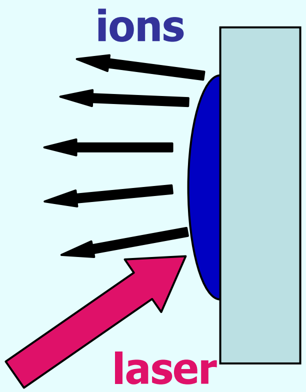

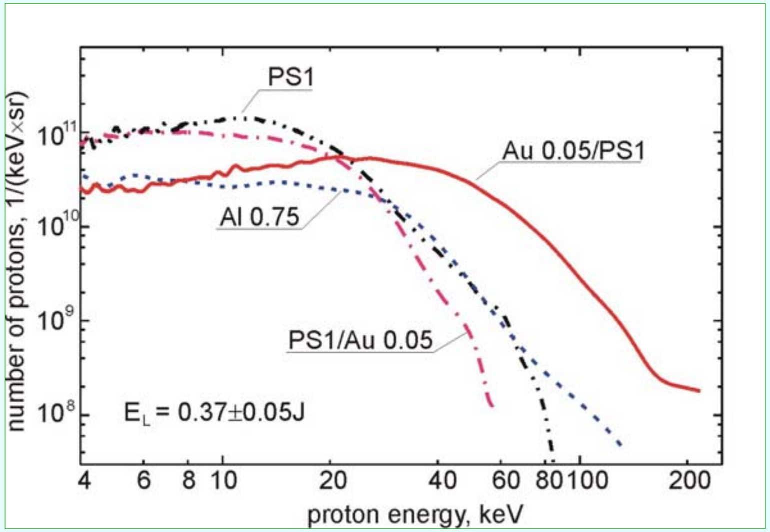

1 J, 1 ps Badziak, JAP, 2004

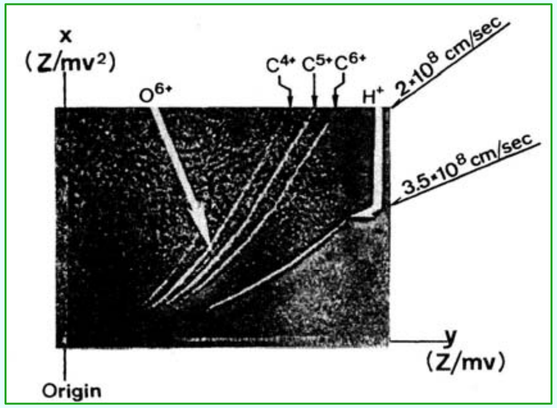

100 J 40 ps, Sakabe et al. PRA 26, 1982

Ion acceleration is a natural result in any laser plasma interactions – formation of a rarefaction wave, but the attractive feature of short pulses is a significant amount of ions with a narrow angular spread and a high energy

Ion emission from the rear side

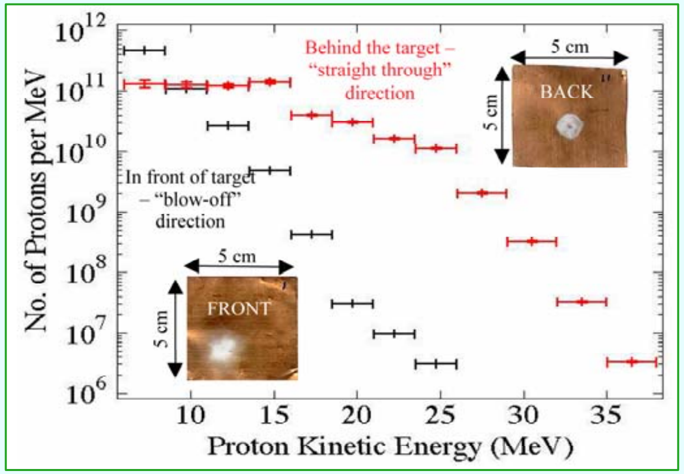

CLF Rutherford 400 J, 1 ps, 2004

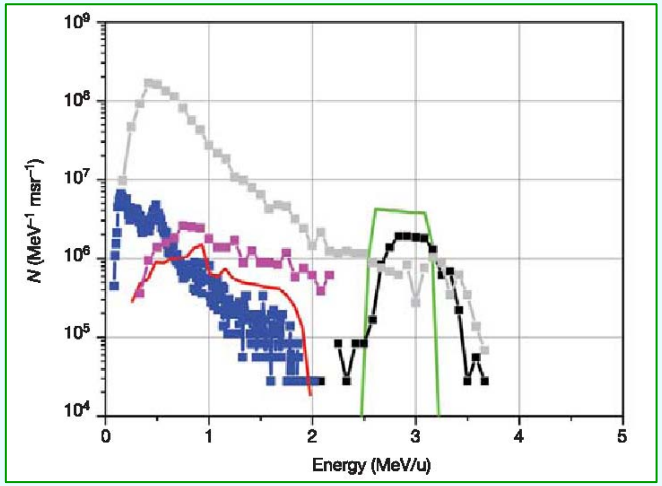

Los Alamos 20 J, 0.6 ps, 2006

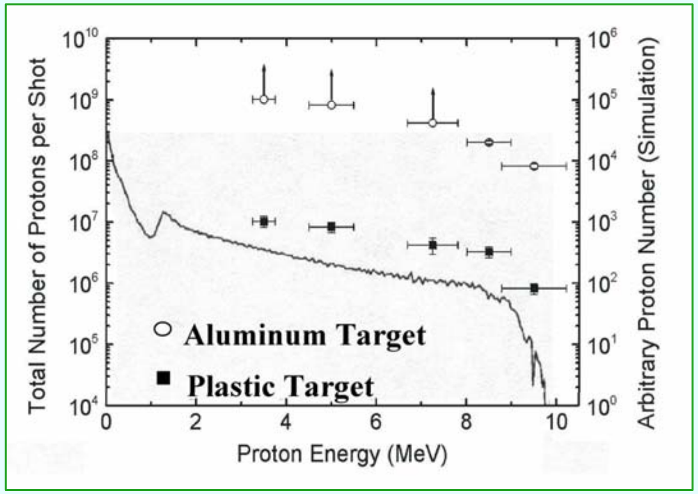

LOA 1 J, 30 fs, 2003

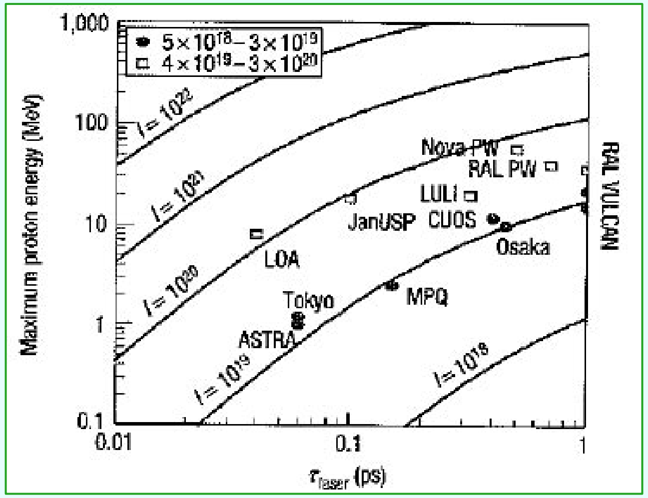

Fuchs et al. Nature Phys., 2006

Attractive features of the rear side ions are their higher energy, small divergence, good laminarity, and good conversion efficiency

Ion acceleration – a basic model

The basic model considers the ion acceleration in the electrostatic field created by hot electrons:

Front side: smooth density profile - small electric field
Rear side: steep density profile - strong electric field, good acceleration

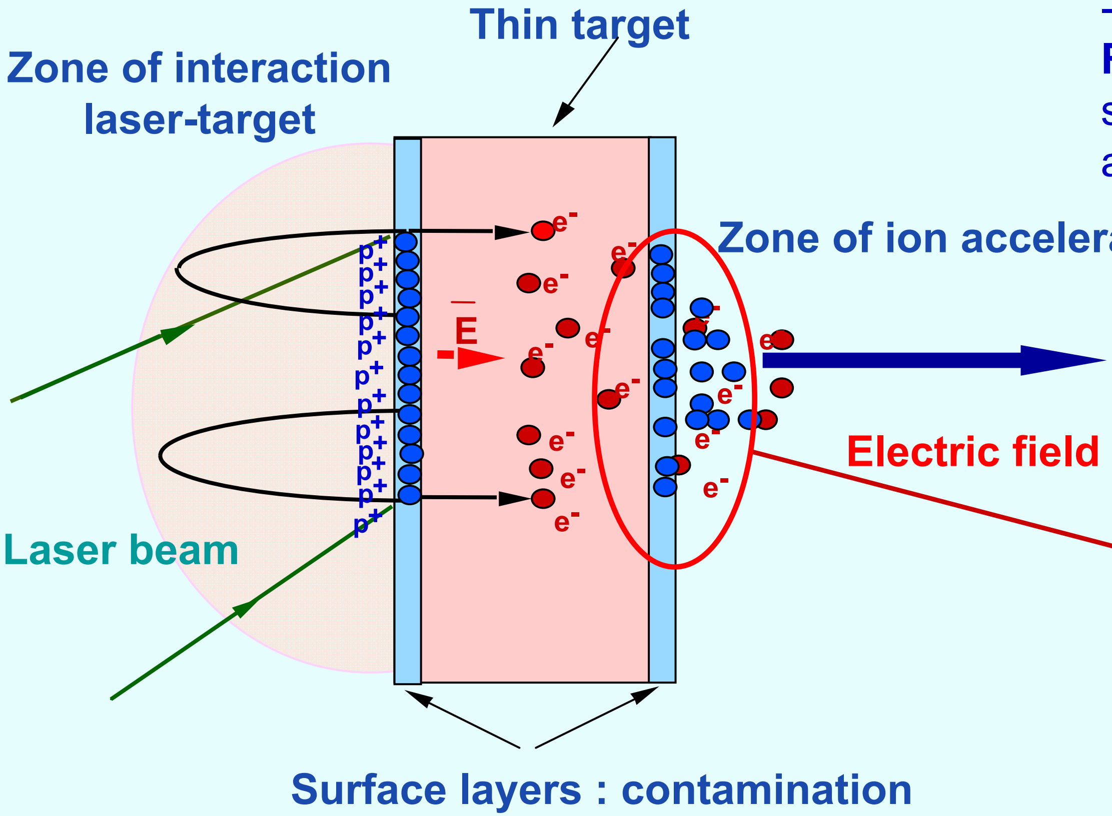

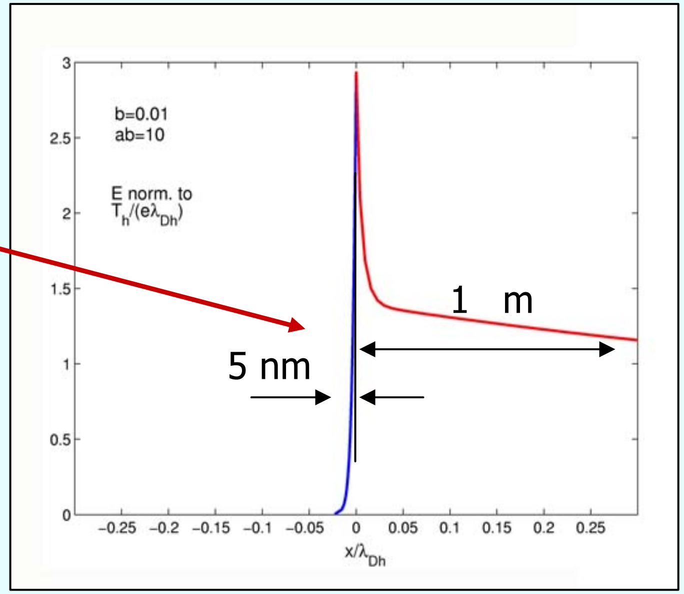

$$T_h \simeq m_e c^2 \left(\sqrt{1 + \tfrac{1}{2} a^2} - 1 \right) \qquad a \simeq 0.9 \sqrt{I_{18} \lambda^2}$$

Quasi-neutral ion acceleration

$$n_e = n_{e0} \exp \frac{e\varphi}{T_e}$$

$$\left(\frac{\partial}{\partial t} + v_i \frac{\partial}{\partial x} \right) n_i = -n_i \frac{\partial v_i}{\partial x}$$

$$\left(\frac{\partial}{\partial t} + v_i \frac{\partial}{\partial x} \right) v_i = -\frac{Ze}{m_i} \frac{\partial \varphi}{\partial x}$$

The basic model of ion acceleration consists of a two-component (electron-ion) plasma with the isothermal electrons and cold collisionless ions coupled by the quasi-neutrality equation:

$$c_s = \sqrt{ZT_e / m_i}$$

$$E = T_h / ec_s t$$

Self-similar solution: Gurevich et al. JETP, 1966

$$n_i = n_{i0} \exp(-x/c_s t - 1), \quad v_i = c_s + x/t, \quad e\varphi = -T_e\,(-x/c_s t - 1)$$

Ion energy spectrum $$dN_i / dv = n_{i0} t \exp(-v / c_s)$$

$$N_i(v) = \int_{-c_s t}^{x(v)} n_i \, dx$$

Maximum ion velocity: electrostatic shock

Quasi-neutral model is in a perfect agreement with the kinetic simulations. However it fails at rarefaction front where

$$L = c_s t \sim \lambda_D$$

$$v_{front} \simeq 2c_s \ln(\tau + \sqrt{\tau^2 + 1})$$

where $\tau = \omega_{pi} t / \sqrt{2e}$ **Mora 2003**

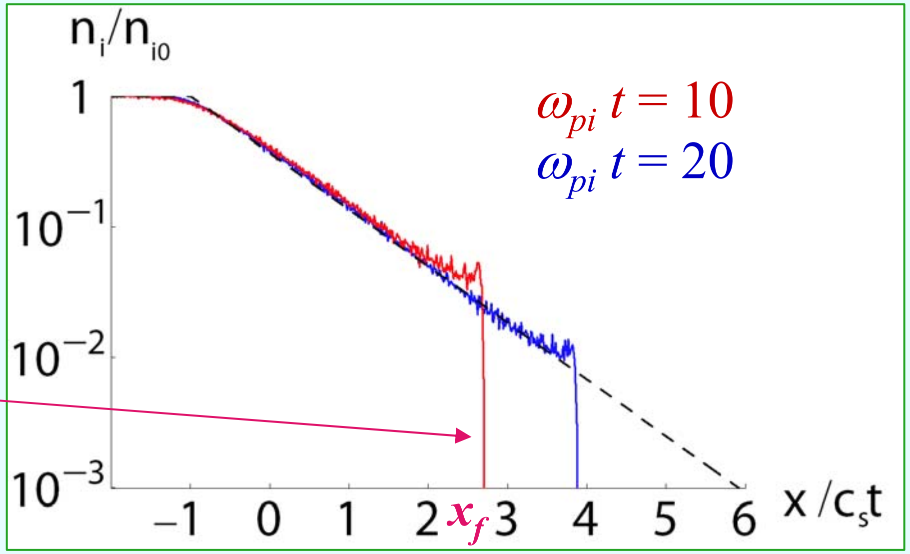

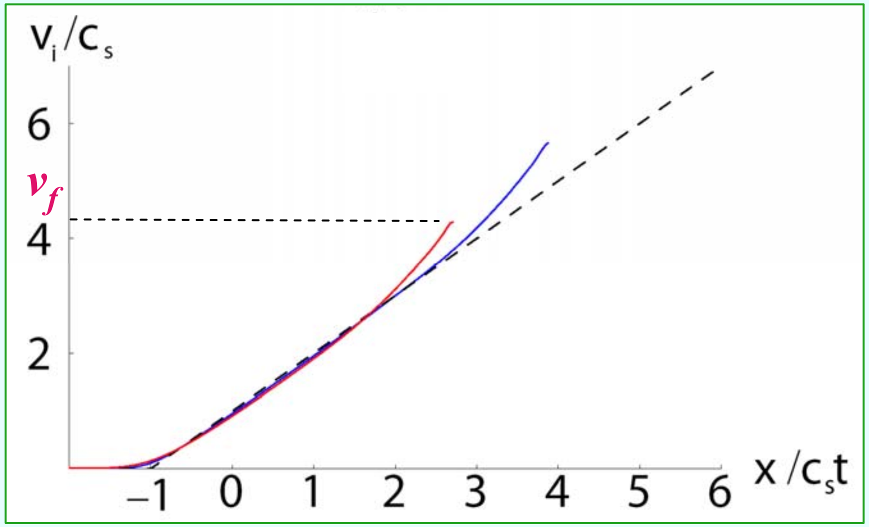

Hybrid simulations: kinetic ions and Boltzmann electrons with a fixed temperature

Tikhonchuk, Pl. Phys. Conf. Fus., 2005

Maximum ion velocity: electrostatic shock

Exponential ion distribution with a high energy cut-off

$$\varepsilon_i \geq ZT_h$$

$$N_{fast} \simeq 0.3Z^{-1} n_{i0} c_s t$$

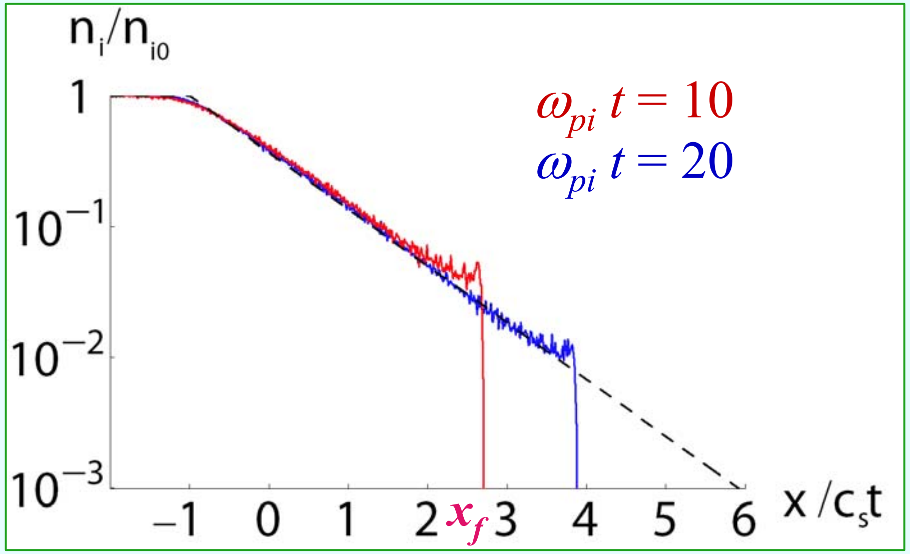

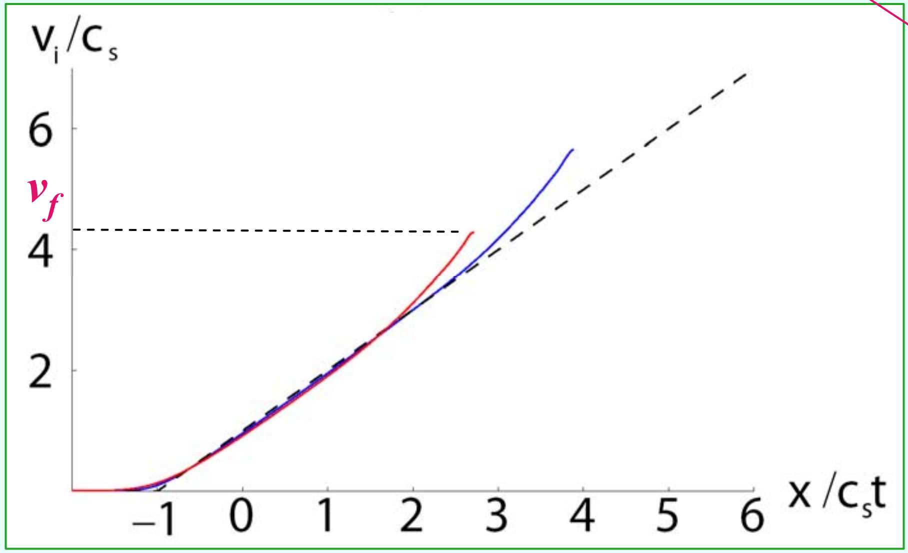

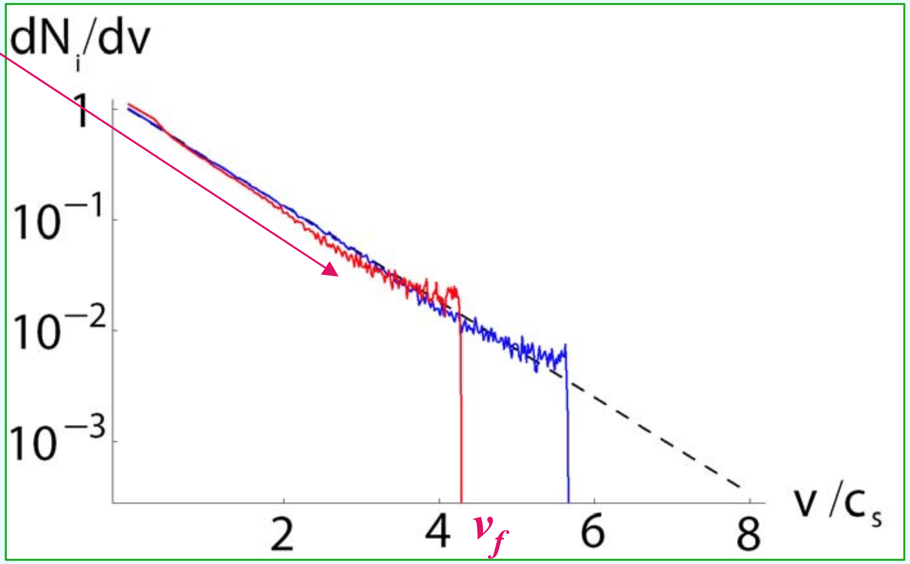

Two temperature electrons: rarefaction shock

A more realistic model has to account for several additional effects:
- two electron populations: cold dominant and hot minority
- ions are created ***in situ*** by the field ionization
- multiple ion species: proton contamination

$$\Delta\varphi \sim 1.3\ T_h$$

Cold electrons are stopped at the shock front
The potential jump at the shock front accelerates ions
Discontinuity appears for $T_h/T_c = 10$: Bezzerides et al. 1978, Wickens 1981

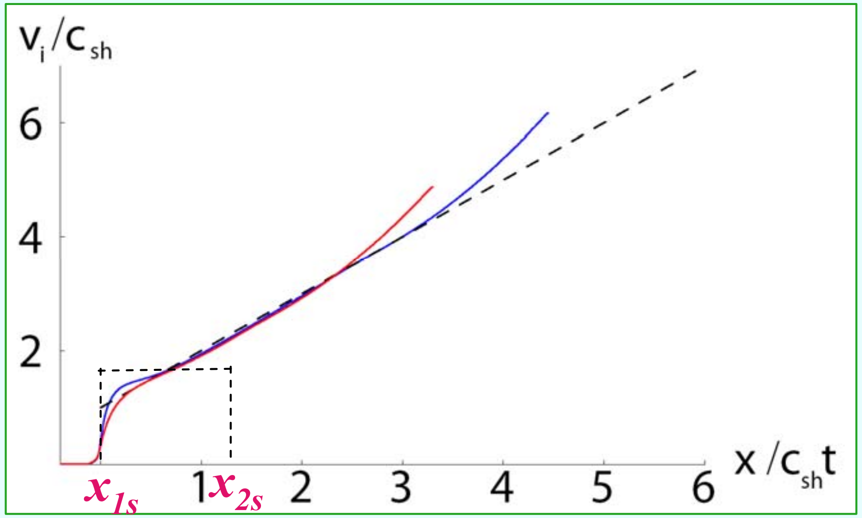

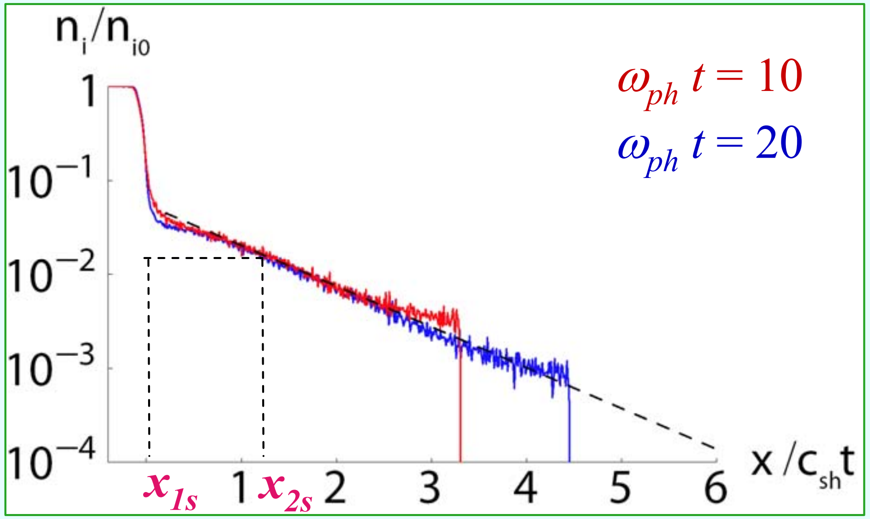

$n_h/n_c = 0.1$, $T_h/T_c = 100$ Tikhonchuk, Pl. Phys. Conf. Fus., 2005

Ion bunching at the shock front

Kinetic hybrid simulations show the collisionless shock and plateau formation

Number ions in the peak

$$N_{peak} = 0.17 Z^{-1} n_{h0} c_{sh} t$$

Number ions in the tail

$$N_{tail} = 0.28 Z^{-1} n_{h0} c_{sh} t$$

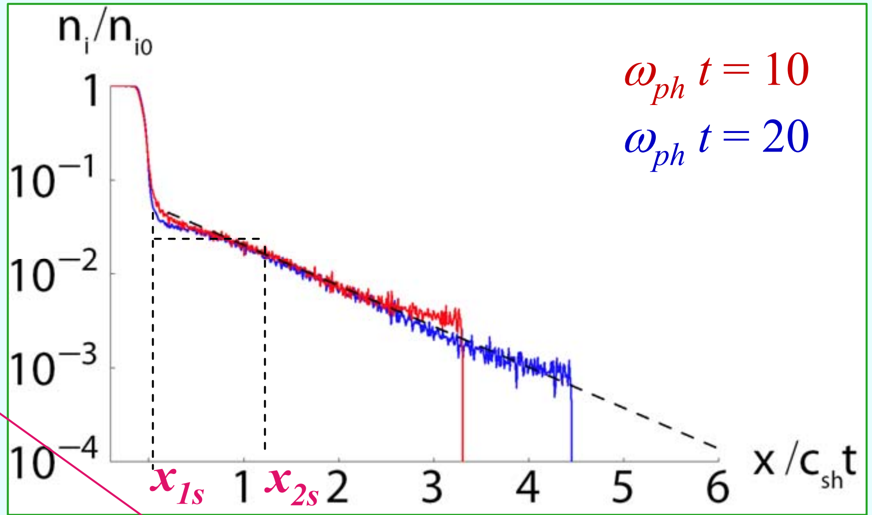

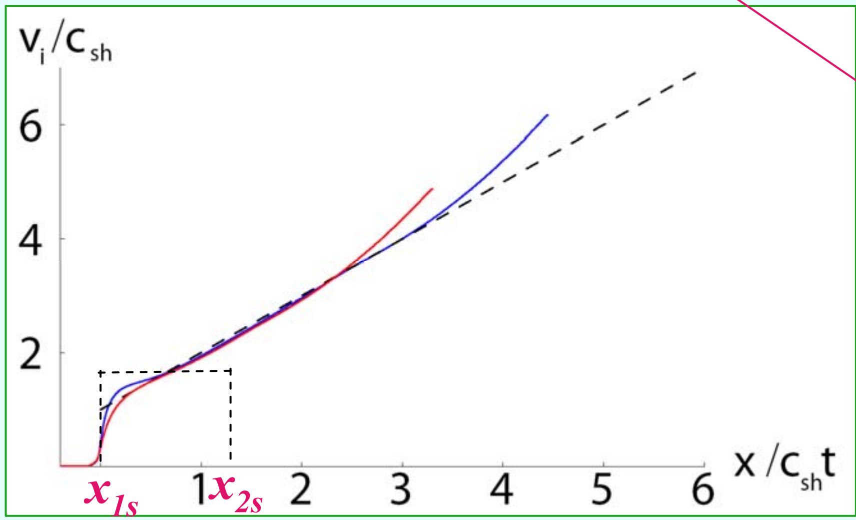

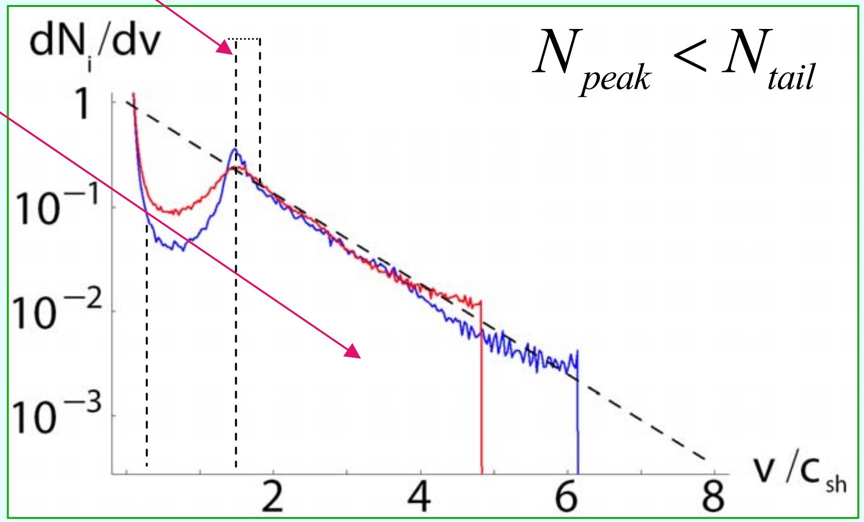

Expansion of two ion species: spatial separation

The ion species separation happens naturally in a homogeneous multi-species targets:

Heavy ion rarefaction wave **Gurevich et al. 1973, Srivastava et al. 1988**

$$v_{k2} = c_{s2}\left[\ln^{1/2}\left(4N\sqrt{2\alpha}\right)+1\right]$$

$C^+/H^+ = 10:1$

Number ions in the peak $N_{peak} = n_{20}c_{s2}t/\sqrt{\alpha}$

Number ions in the tail $N_{tail} = n_{20}c_{s2}t$

$$\alpha = \frac{A_1 Z_2}{A_2 Z_1} \gg 1 \qquad N = \frac{Z_1 n_{10}}{Z_2 n_{20}}$$

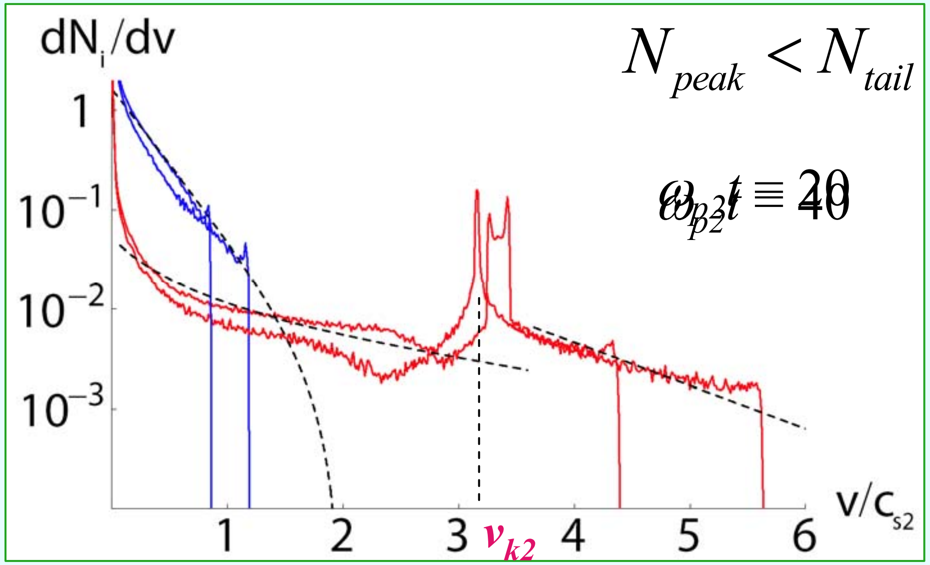

Tikhonchuk, Pl. Phys. Conf. Fus., 2005

Kinetic simulations of two-ion-species expansion

Simulations show the formation of the plateau region in velocity behind the separation point

$$x_{k1} = c_{s1} t \ln\left(4N\sqrt{2\alpha}\right)$$

$$x_{k2} = c_{s2} t \ln^{1/2}\left(4N\sqrt{2\alpha}\right)$$

$$\alpha = \frac{A_1 Z_2}{A_2 Z_1} \gg 1 \qquad N = \frac{Z_1 n_{10}}{Z_2 n_{20}}$$

Heavy ion shock front

$$\Delta\varphi \sim 4.5\, T_h$$

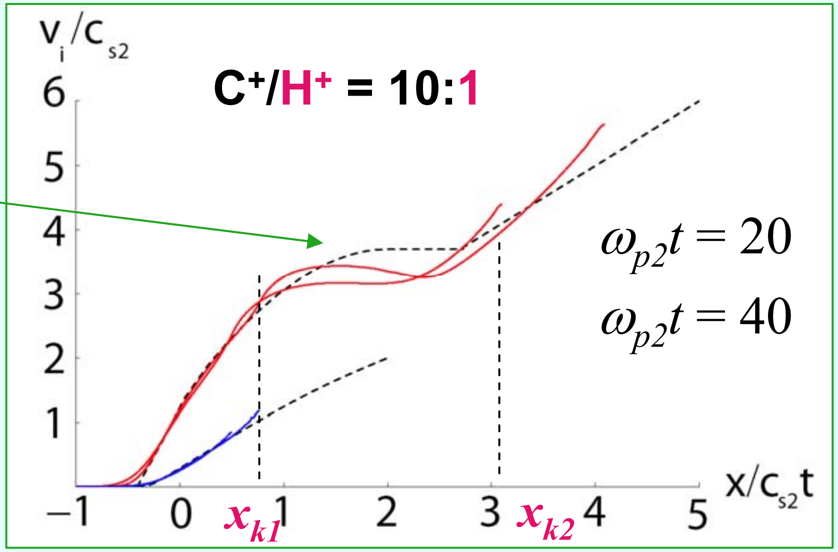

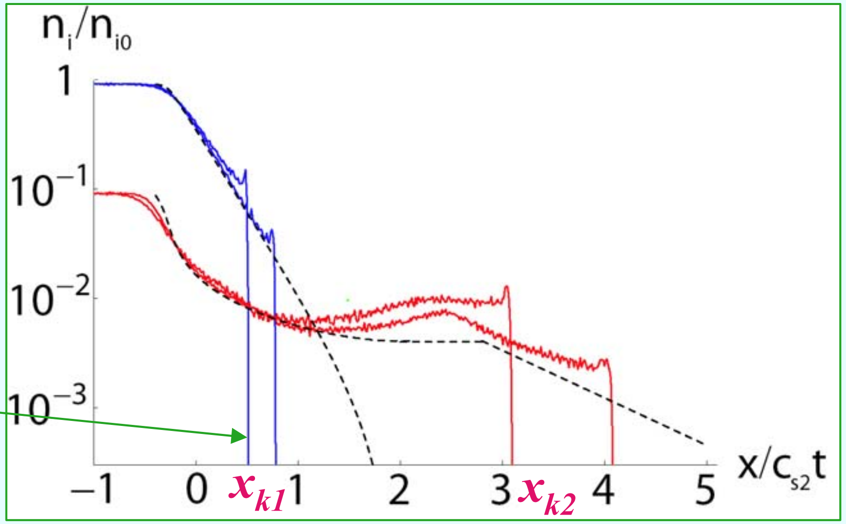

Experiment on ion acceleration from water droplets

Formation of peaks and holes in the ion energy spectrum has been seen in the experiment: liquid water droplets are the unique targets with two ion species and without surface contamination. The idea of light ions accelerated in the heavy ion front was verified with H_2O and D_2O targets

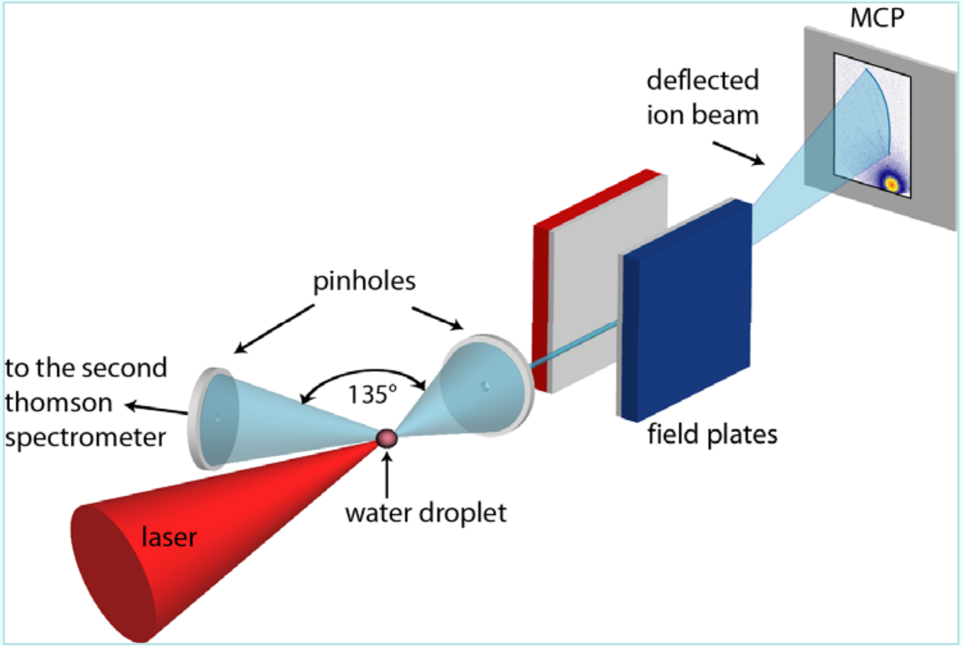

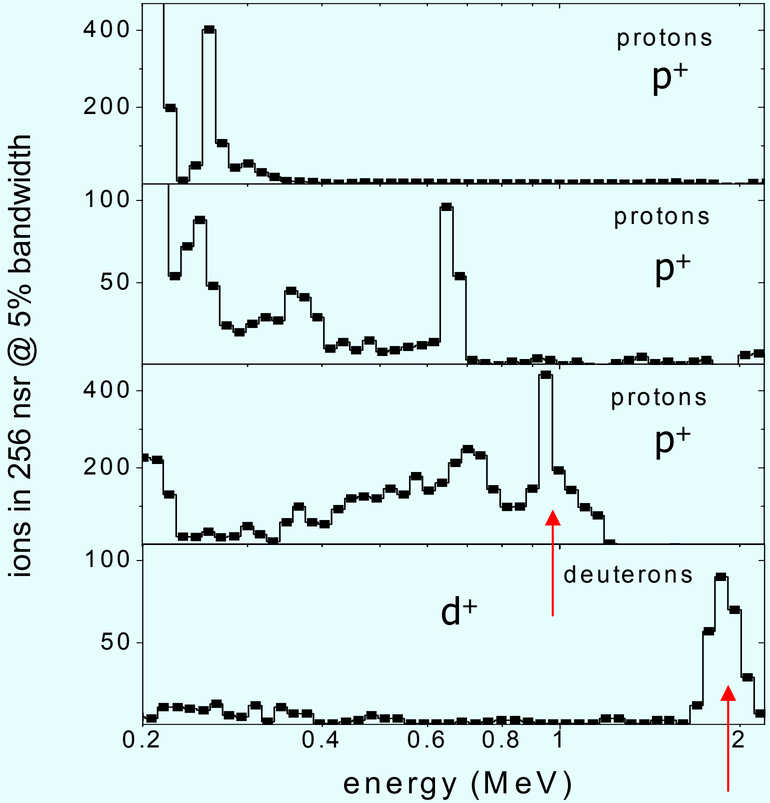

Two times difference in the deuteron and proton energies they are accelerated to the same velocity

Brantov et al. Phys. Plasmas, 2006

Two ion species: heterogeneous target

Similar interaction between two ion species takes place in a heterogeneous target

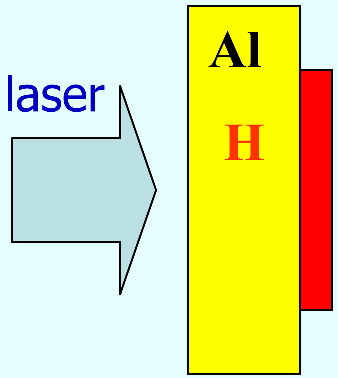

Esirkepov et al. PRL, 2002
Brantov et al. Phys. Plasmas, 2006
Formation of a narrow ion spectrum in a heterogeneous target

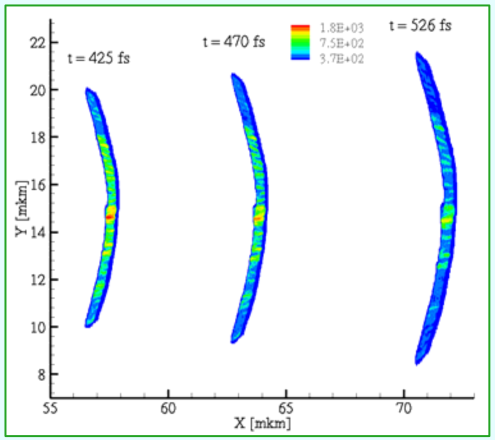

low density hydrogen 10^{20} cm^{-3}

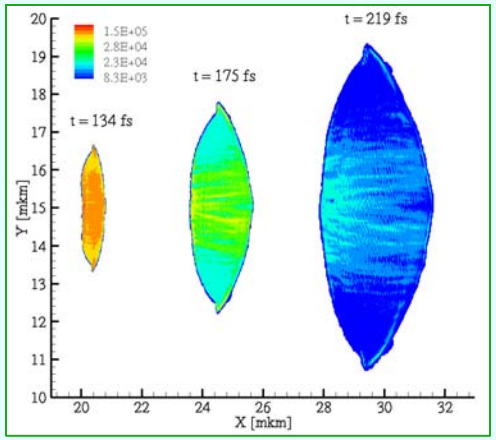

high density hydrogen 10^{22} cm^{-3}

Two ion species: heterogeneous target

Light ions in a heterogeneous target indeed are moving initially in a narrow bunch, however, a narrow spectrum spreads with time - this is the effect of Coulomb explosion: Full PIC simulations 1D

Laser: 1 μm, 4×10^{19} W/cm^2, 50 fs **Target: 3 μm Al + 0.1 μm H**

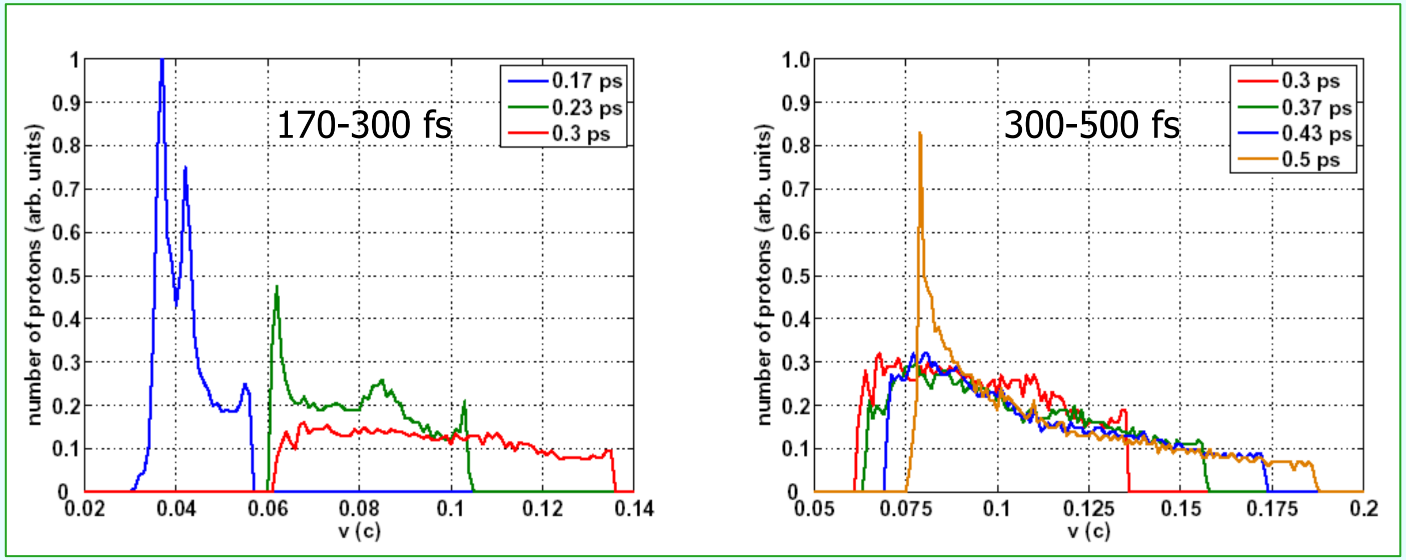

Simulations show that heavy ions are following the protons closely and affect their acceleration at later times: Brantov et al. Phys. Plasmas, 2006

Comparison: homogeneous and double layer target

3D simulations of the ion acceleration from a foil: comparison of the homogeneous two-species target and a double layer target – protons are gaining the same energy

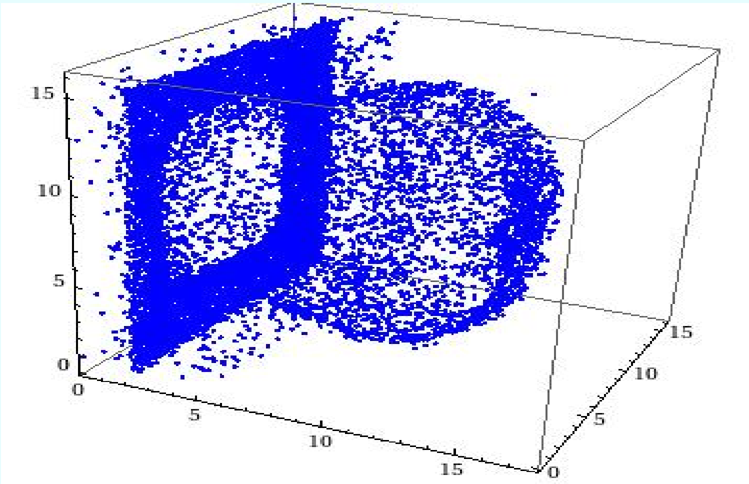

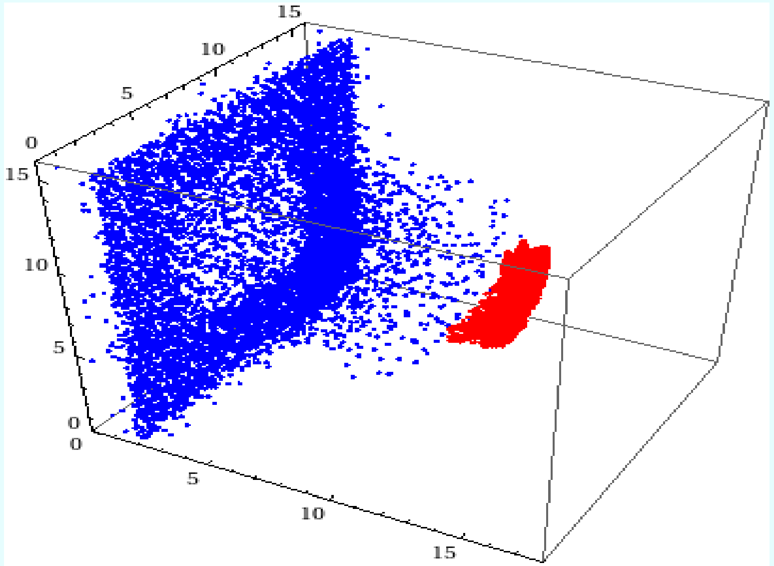

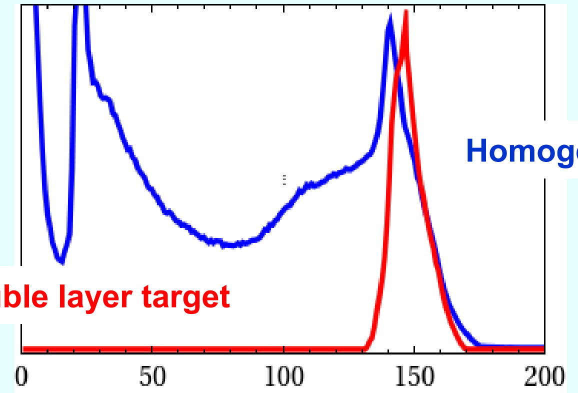

Brantov et al., 2009

I =5×10^{21} W/cm^2 super-Gaussian profile in perpendicular directions with FWHM = 4 μm τ = 30 fs

Radiation pressure ion acceleration

Radiation pressure acceleration at the front side and in the volume of target:
- cold electrons (circ polarization)
- high quality laser pulse (very high contrast > 10^{12})
- higher intensities (> 10^{21} W/cm^2)
- mild restrictions on the target
- could be more efficient
- more ions could be accelerated

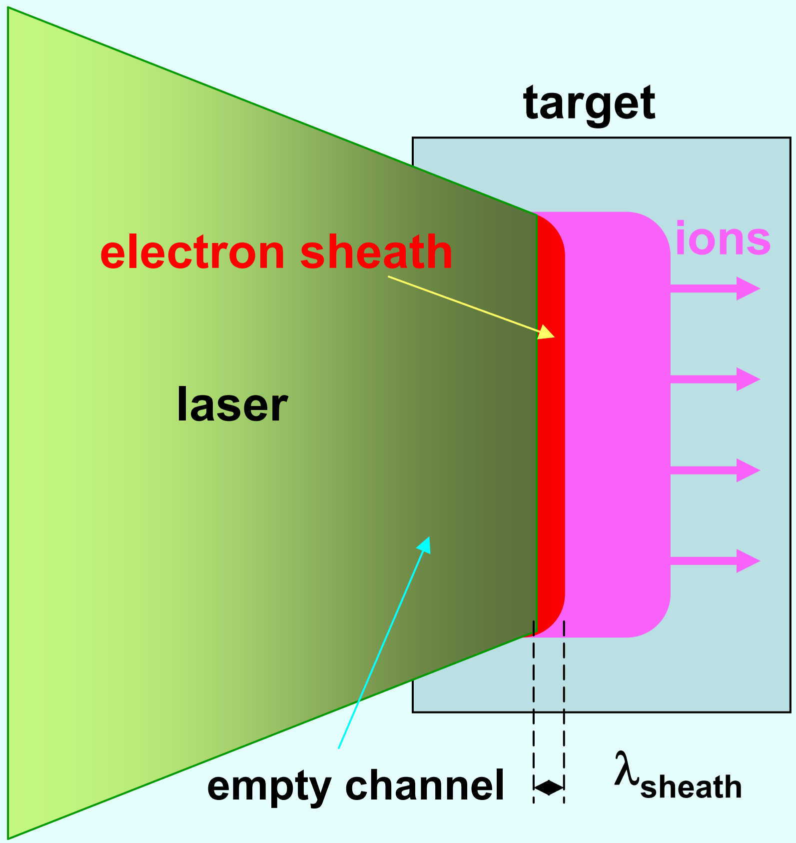

Circular *vs* linear laser polarization

Circular laser polarization suppresses the electron heating. It provides favorable conditions for ponderomotive acceleration and ion beam neutralization. Example of electron spectra at the laser intensity 1.5×10^{20} W/cm^2 and a solid density.

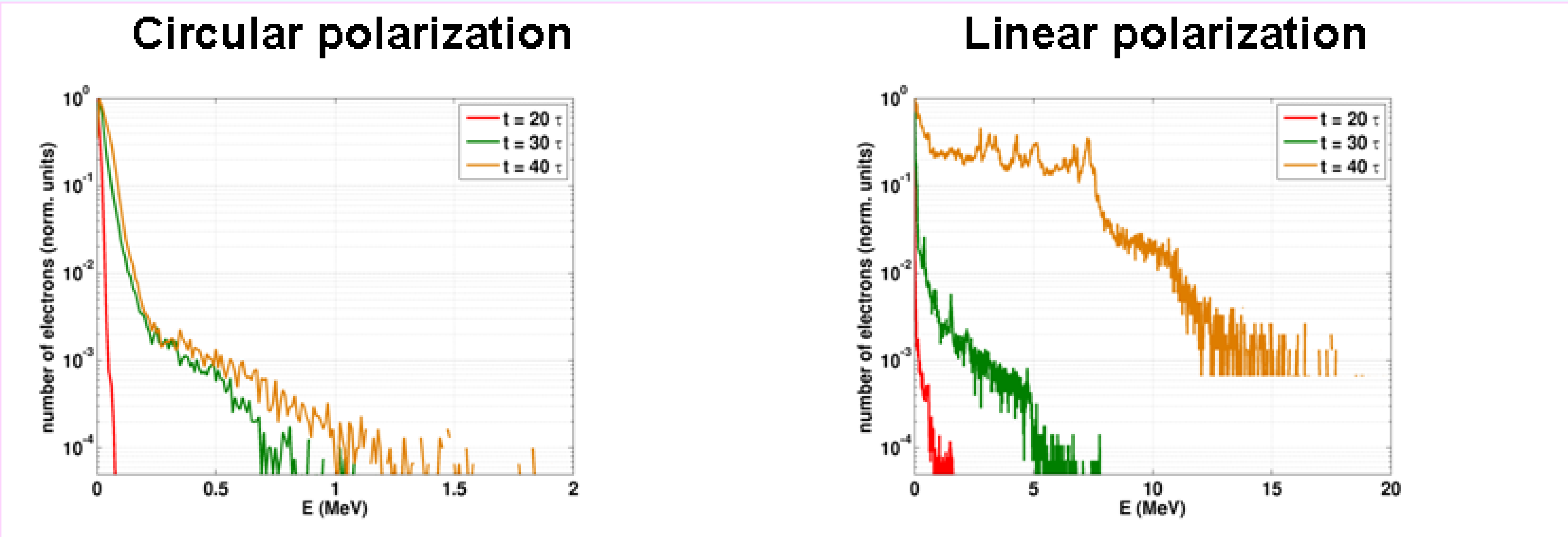

Cold electrons **Hot electrons**

Klimo, PRST-AB, 2008

Circular laser polarization and electron radiation losses are two main effects to maintain a low electron temperature

Ion acceleration by the laser piston: the piston velocity

Conservation of the momentum (pressure) in the piston reference frame: stationary propagation

$$2\frac{I_{\text{las}}}{c}\frac{1-\beta_f}{1+\beta_f}=2\rho_0\gamma_f^2\beta_f^2c^2$$

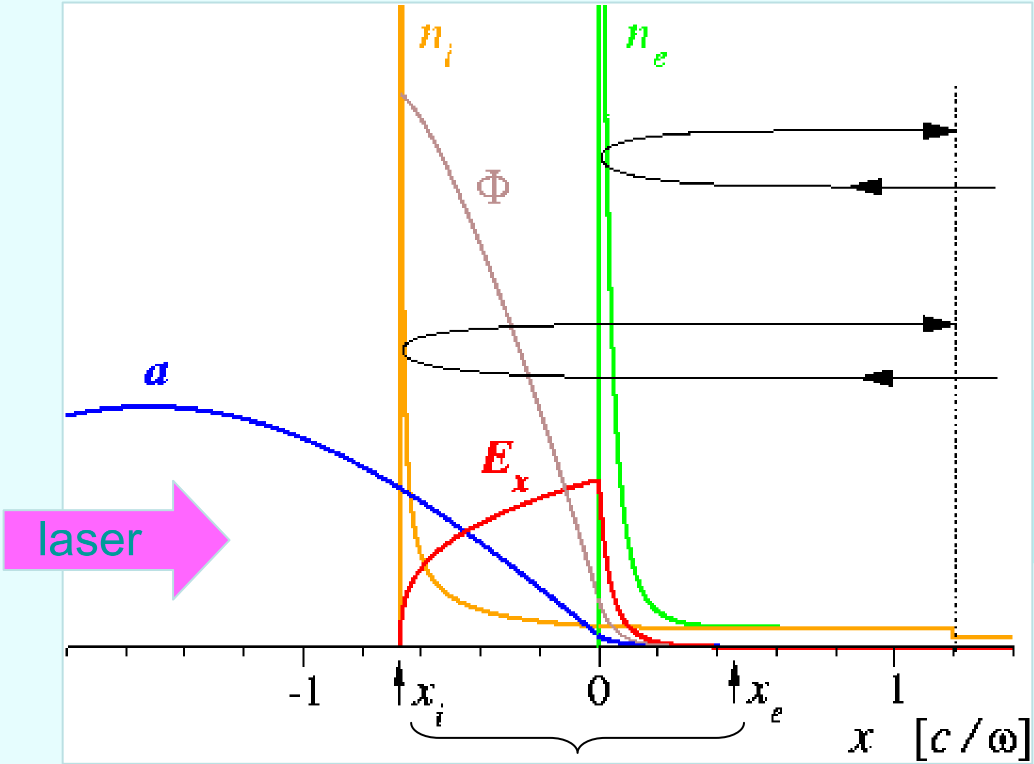

charge separation layer

piston velocity $v_f = \beta_f c$

$$\beta_f=\frac{\sqrt{I_{\text{las}}}}{\sqrt{I_{\text{las}}}+\sqrt{\rho c^3}}$$

ion energy and the efficiency of ion acceleration are defined by the piston velocity

$$\varepsilon_i=2m_ic^2\beta_f^2\gamma_f^2 \qquad 1-R=\frac{2\beta_f}{1+\beta_f}$$

Naumova et al., PRL, 102, 2009, Robinson et al., PPCF, 51, 2009

Structure of the charge separation layer: electrostatic field and ion density distribution

The electrostatic field profile in the charge separation layer follows from the Poisson equation ($n_e = 0$)

$$\frac{d^2\Phi'}{dz'^2} = -\frac{Zen_i'}{\varepsilon_0}$$

and the ion energy and mass conservation in the piston reference frame:

$$Ze\Phi' + \varepsilon_i' = m_i c^2\left(\gamma_f - 1\right); \qquad n_i' = 2n_0\gamma_f \frac{\mathrm{v}_f}{\mathrm{v}_i'}$$

The first integral defines the electric field strength:

$$\frac{d\gamma_i'}{dz'} = 2\frac{\omega_{pi}}{c}\sqrt{\beta_f\gamma_f}\left(\gamma_i'^2 - 1\right)^{1/4}$$

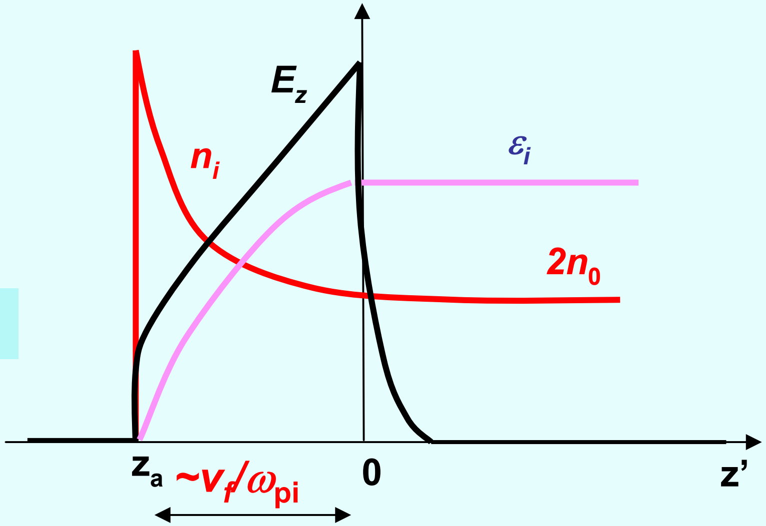

$$E_{z\max} \simeq 2E_{\mathrm{las}}\sqrt{\frac{1-\beta_f}{1+\beta_f}}$$

Thickness of the ion charge separation layer

The thickness of the ion charge separation layer is proportional to the piston velocity

$$\Delta z_i = \frac{c}{2\omega_{pi}}\sqrt{\frac{\gamma_f}{\beta_f}}\int_1^{\gamma_f}\frac{d\gamma_i'}{\left(\gamma_i'^2-1\right)^{1/4}}$$

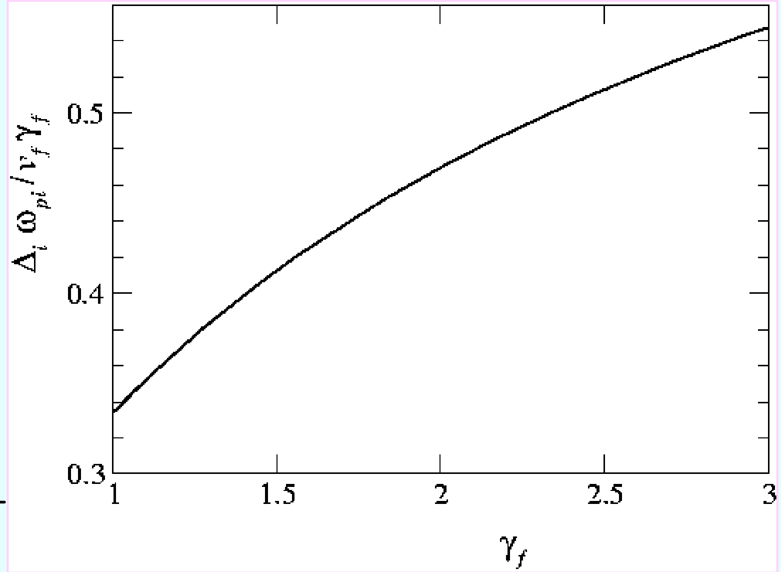

if $\beta_f \ll 1$

$$\Delta z_i \simeq \frac{a_0 c}{3\omega_0}\frac{n_c}{n_0}$$

while for the immobile ions

$$\Delta z_i \simeq \frac{2a_0 c}{\omega_0}\frac{n_c}{n_0}$$

The time of ion circulation is independent on the laser intensity

$$\Delta t_i = \frac{1}{\omega_{pi}}\sqrt{\frac{\gamma_f}{\beta_f}}\int_1^{\gamma_f}\frac{\gamma_i' d\gamma_i'}{\left(\gamma_i'^2-1\right)^{3/4}} \simeq \frac{2\gamma_f}{\omega_{pi}}$$

This time of ion circulation coincides exactly with the period of piston velocity oscillations found in the PIC simulations

Structure of the charge separation layer: laser field and electron density distribution

The electrostatic field profile in the charge separation layer follows from the Poisson equation

$$\frac{d^2\Phi'}{dz'^2} = -e\frac{Zn_i' - n_e'}{\varepsilon_0}$$

and the electron energy and mass conservation in the piston reference frame:

$$-e\Phi' + \varepsilon_e' = m_e c^2\left(\gamma_f - 1\right); \qquad n_e' = 2Zn_0\gamma_f \frac{\mathrm{v}_f}{\mathrm{v}_e'}$$

$$\frac{d^2\gamma_e'}{d\zeta^2} = 2\gamma_f\beta_f\frac{n_0}{n_c}\left(\frac{Z\gamma_e'}{\sqrt{\gamma_e'^2 - 1 - a^2}} - \frac{\gamma_i'}{\sqrt{\gamma_i'^2 - 1}}\right)$$

$$\frac{d^2 a}{d\zeta^2} = 2\gamma_f\frac{n_0}{n_c}\frac{Z\beta_f a}{\sqrt{\gamma_e'^2 - 1 - a'^2}} - \frac{1-\beta_f}{1+\beta_f}a$$

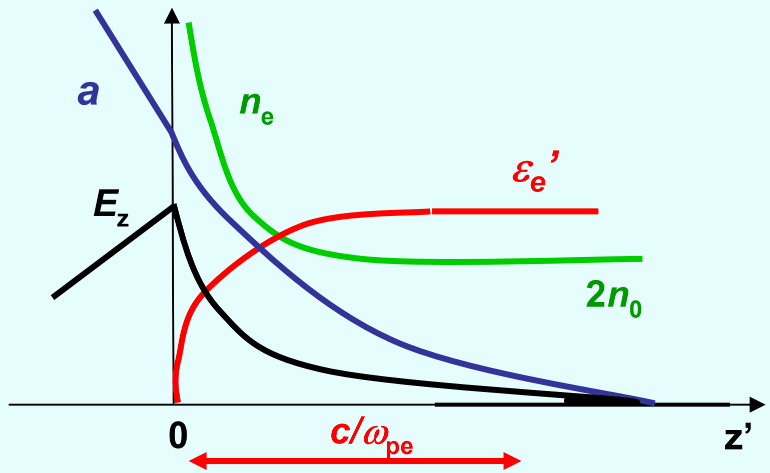

$$\left(\frac{da}{d\zeta}\right)^2_{\zeta=0} + a^2_{\zeta=0} \simeq 4a_0^2\frac{1-\beta_f}{1+\beta_f}$$

The electron layer thickness c/ω_{pe} the laser field

Laser amplitude in the electron charge separation layer

Laser amplitude on the board of the electron charge separation layer *a*(0) is adjusted self-consistently in such a way that the ponderomotive force is equal to the electric force: $F_{pf} = e\,E_{z\,max}$
It decreases slowly with the plasma density

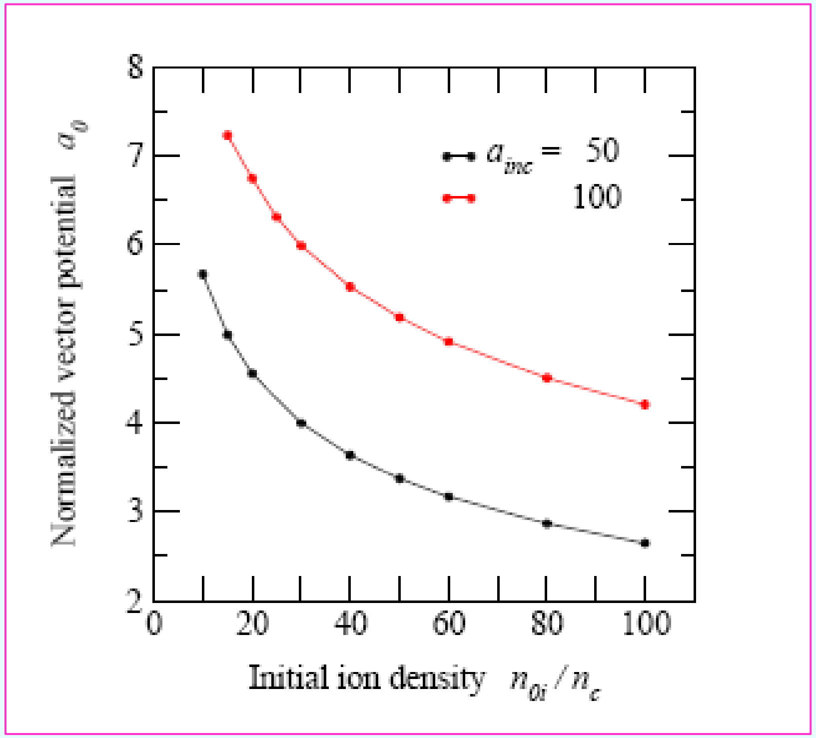

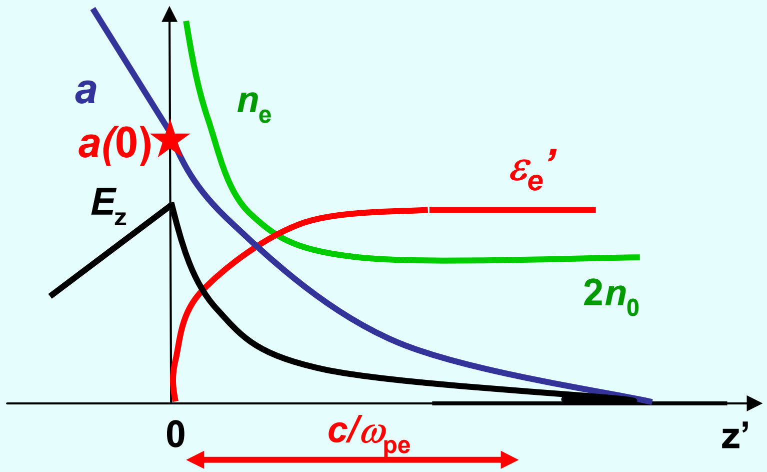

A very tight balance between the ponderomotive potential and the electrostatic field can make the electron confinement unstable

Schlegel, Phys. Plasmas, 2009

Electron radiation and slowing down

Thomson scattering is strongly amplified in the relativistic laser field due to the high order harmonic generation:

if $\gamma_e << a$

$$\omega_{\max} \simeq \omega a^3 \quad P_{\text{rad}} \cong \frac{e^2\omega^2}{6\pi\varepsilon_0 c} a^4$$

if $\gamma_e >> a$

$$\omega_{\max} \simeq 4\omega a \gamma_e^2 \quad P_{\text{rad}} \cong \frac{2e^2\omega^2}{3\pi\varepsilon_0 c} \gamma_e^2 a^2$$

Esarey et al., Phys. Rev. E 48, 1993

Radiation is enhanced if the electron propagates toward the laser beam with a high energy, $\gamma_e >> a >> 1$.

The photons with the frequencies $\omega_{ph} \sim \omega a \gamma_e^2$ are emitted in a narrow cone $\theta \sim a/\gamma_e << 1$.

The electron radiation stopping length

$$l_{\text{rad}} \simeq \frac{c^2}{r_e \omega^2} \frac{1}{\gamma_e a^2} \simeq \frac{1}{40} \frac{\lambda^2}{r_e a^4} \frac{n_0}{n_c} \sim 3 - 5\ \mu\text{m}$$

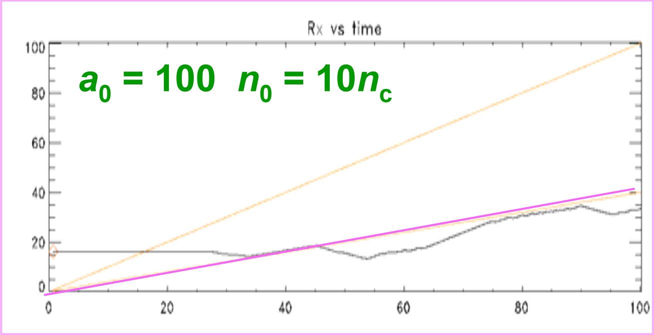

for n_0/n_c = 40, a = 100 electrons are confined behind the piston

Radiation losses can be significant for laser amplitudes a > 100 and for linear polarization

Ion energy spectrum in inhomogeneous plasma

Ions are mono-energetic in a homogeneous plasma, in an exponential density profile the ions are a power spectrum

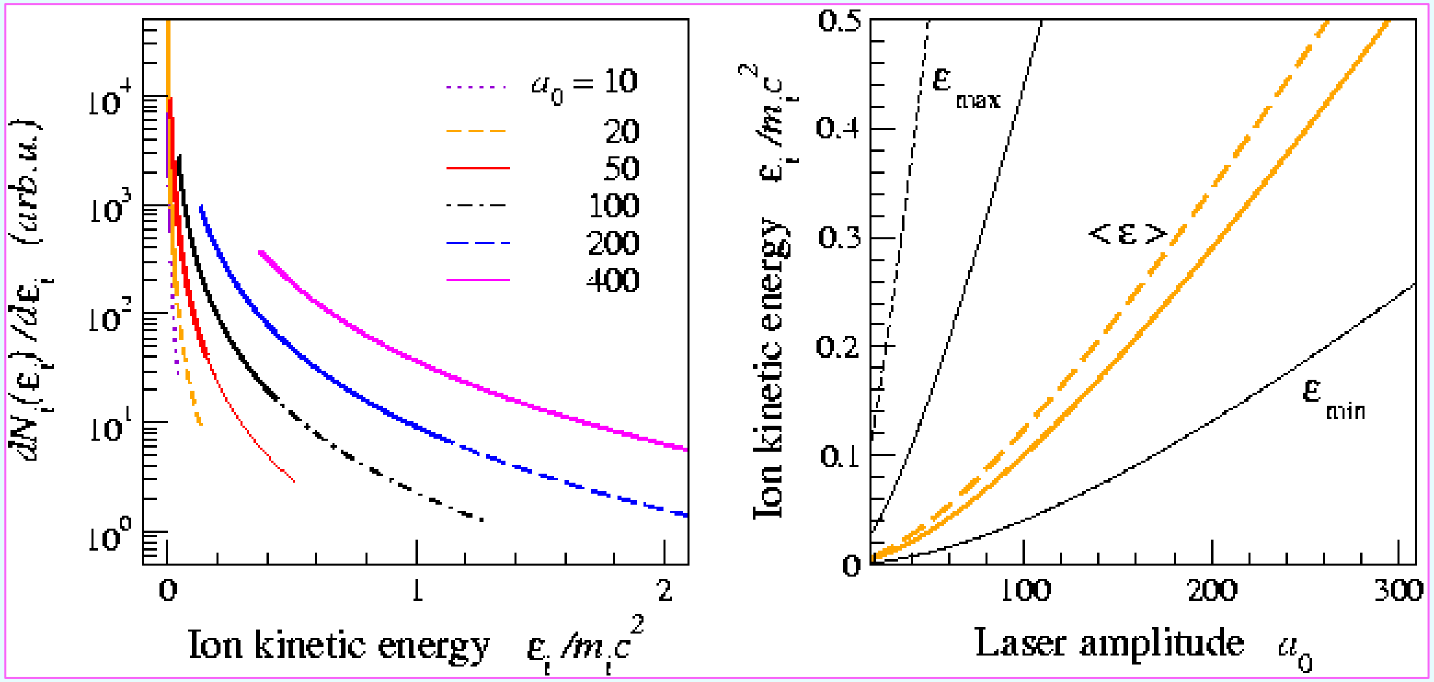

Deuteron spectra in a plasma with the density increasing from 1 to 100n_c

$$\frac{dN_i}{d\varepsilon} = \frac{I_{las}L}{2m_i^2c^5}\frac{1}{\beta_f^4\gamma_f^6\left(1+\beta_f\right)}$$

$$\left\langle \varepsilon_i \right\rangle = \frac{4I_{las}}{n_{i\max}c}\ln\frac{\beta_{f\min}}{\beta_{f\max}}$$

Time of hole boring and laser fluence

Analytical formulas provide the scalings for design of the fast ignition parameters

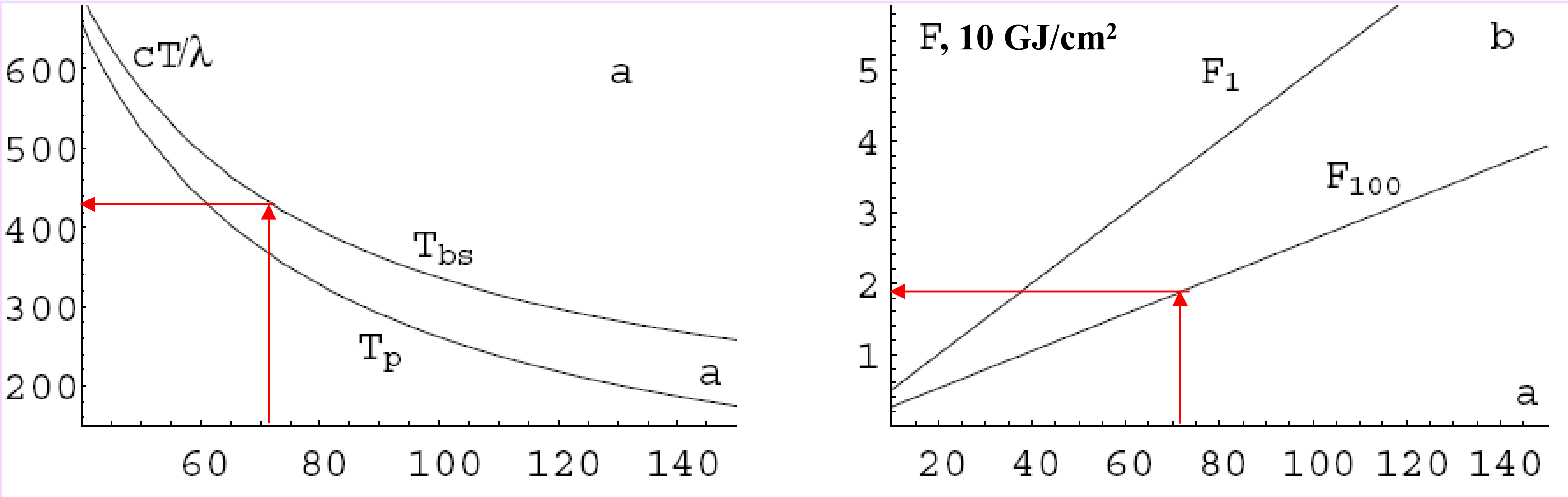

$F_{100} = I_{inc}T_p$ is the laser flux needed for accelerate ions from the density increasing from 1 to 100n_c over the length of 100λ, F_1 is the same for the density range 0.1 to 1n_c over the length of 1000λ

$$T_p = \sqrt{\frac{c}{I_{\text{las}}}}\int\frac{L\mathrm{d}\rho}{\sqrt{\rho}}$$

$$F_{\text{las}} = \sqrt{cI_{\text{las}}}\int\frac{L\mathrm{d}\rho}{\sqrt{\rho}}$$

$$F_i \approx \frac{1}{m_i}\int L\varepsilon_i(\rho)\mathrm{d}\rho$$

1D & 2D PIC simulations of ion acceleration & hole boring

Series of 1D simulations was dedicated to validation of the ion acceleration model in homogeneous and inhomogeneous plasmas

2D simulations in a plasma with exponential profile were dedicated to the analysis of the ion energy distribution and divergence in function of the laser intensity distribution

Laser pulse:

a_0 = 100
circularly polarized
$I_0 = 4\times10^{22}$ W/cm^2
$\tau = 188\ \lambda/c$
2D: d/λ = 20 flat-top
with exp. wings

Plasma: deuterium
exponential profile
L/λ = 20 n_0/n_c = 5 – 100

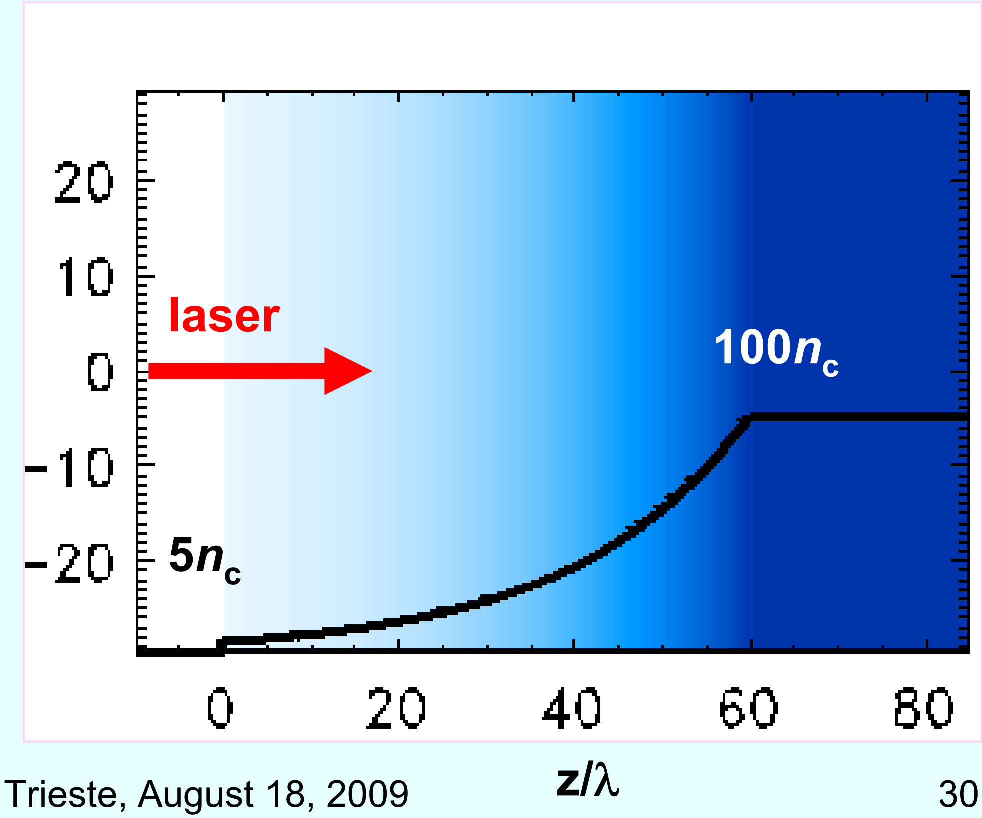

Numerical modeling of the electron radiation losses

The code accounts for the electron radiation in the laser field and for the electron slowing down due to the radiation emission

I.V. Sokolov, *Re-normalization in the Lorentz-Abraham-Dirac equation for radiation force in classical electrodynamics*, JETP 108 (2009)

I.V. Sokolov, N.M. Naumova, J.A. Nees, G.A. Mourou, V.P.Yanovsky, *Dynamics of Emitting Electrons in Strong Electromagnetic Fields*, arXiv:0904.0405

The electron motion is described by the modified Lorentz-Abraham-Dirac equation, which conserves electron energy and momentum

$$\frac{d\mathbf{p}_e}{dt} = \mathbf{f}_L - e\delta\mathbf{v}_e \times \mathbf{B} - \frac{\mathbf{v}_e}{c^2} P_{rad} \qquad \frac{d\mathbf{x}_e}{dt} = \mathbf{v}_e + \delta\mathbf{v}_e$$

$$\mathbf{f}_L = -e\left(\mathbf{E} + \mathbf{v}_e \times \mathbf{B}\right) \qquad \mathrm{P}_{rad} = \gamma_e^2 \delta\mathbf{v}_e \cdot \mathbf{f}_L$$

The emission of each electron is supposed to be incoherent, its motion is approximated by a fraction of a circle at each time step, assuming $\delta v_e << v_e$

$$\delta\mathbf{v}_e = \frac{\tau_0}{m_e} \frac{\mathbf{f}_L - \mathbf{v}_e\left(\mathbf{v}_e \cdot \mathbf{f}_L\right)/c^2}{1 + \tau_0\left(\mathbf{v}_e \cdot \mathbf{f}_L\right)/m_e c^2} \qquad \tau_0 = \frac{\mu_0 e^2}{6\pi m_e c} \qquad \omega_{rot} = \left|\mathbf{p}_e \times \mathbf{f}_L\right| / \mathbf{p}_e^2$$

emission frequency $\omega \sim \omega_{rot}^3$

Example of 1D PIC simulation: circular polarization

Lower intensity: $a_0 = 20$, $I_0 = 1.6\times10^{21}$ W/cm^2 $n_0 = 20\ n_c$

Estimates: $1 - R = 0.129$ $\beta_f = 0.07$ $T_b = 93T_0$
$eE_z/m_e\omega_o c = 37$ $p_i/m_i c = 0.14$ $\varepsilon_i = 18$ MeV

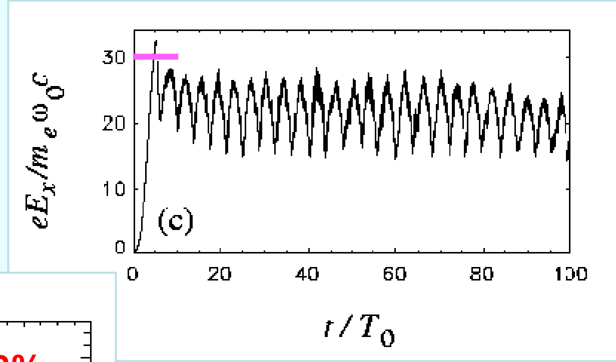

electric field oscillations

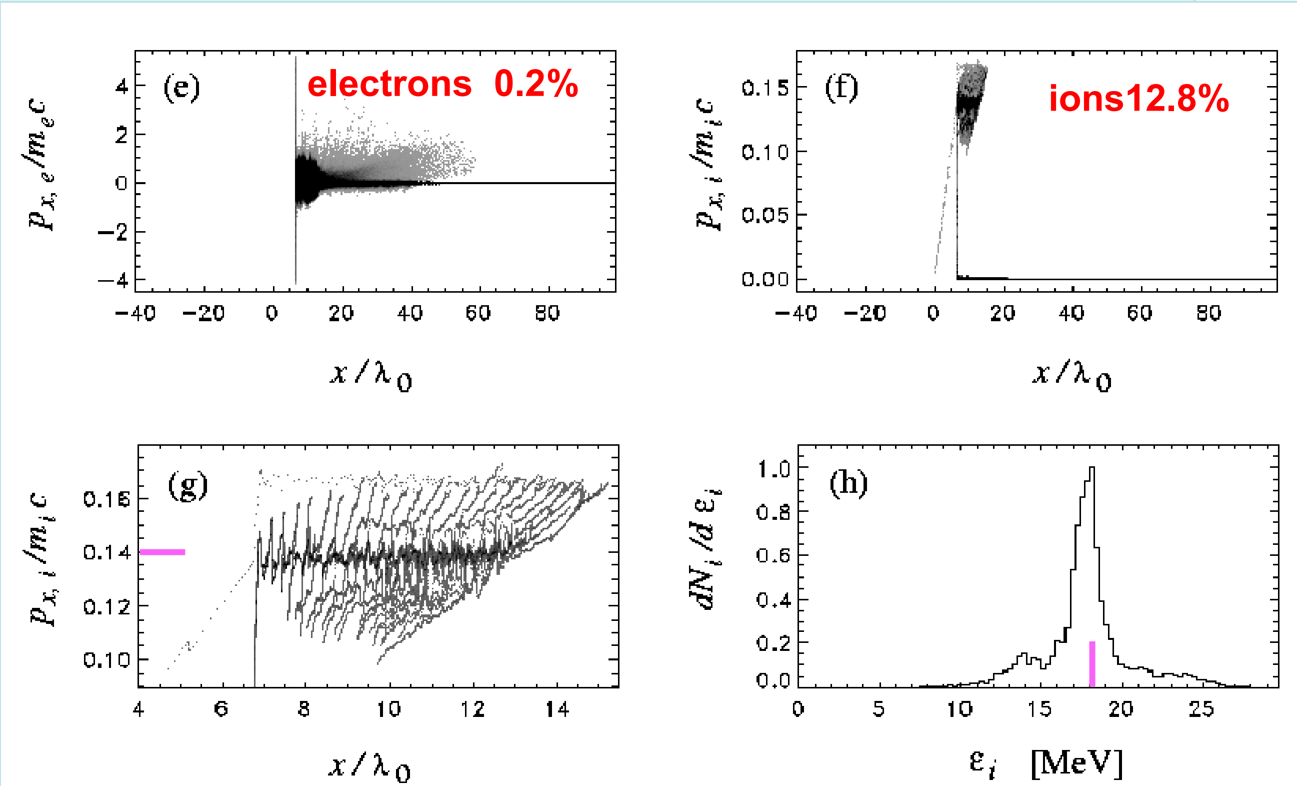

This is a reference case where we find rather good agreement of numerical results with the theoretical model. No electrons escape the piston, small energy spread of accelerated ions ~ 10%, small radiation losses < 0.1%

Schlegel, Phys. Plasmas, 2009

Example of 1D PIC simulation: circular polarization

High intensity: $a_0 = 100$, $I_0 = 4\times10^{21}$ W/cm^2 $n_0 = 20\ n_c$

$1 - R = 0.425$ $\beta_f = 0.27$ $T_b = 93T_0$ $eE_z/m_e\omega_o c = 150$ $p_i/m_i c = 0.58$ $\varepsilon_i = 300$ MeV

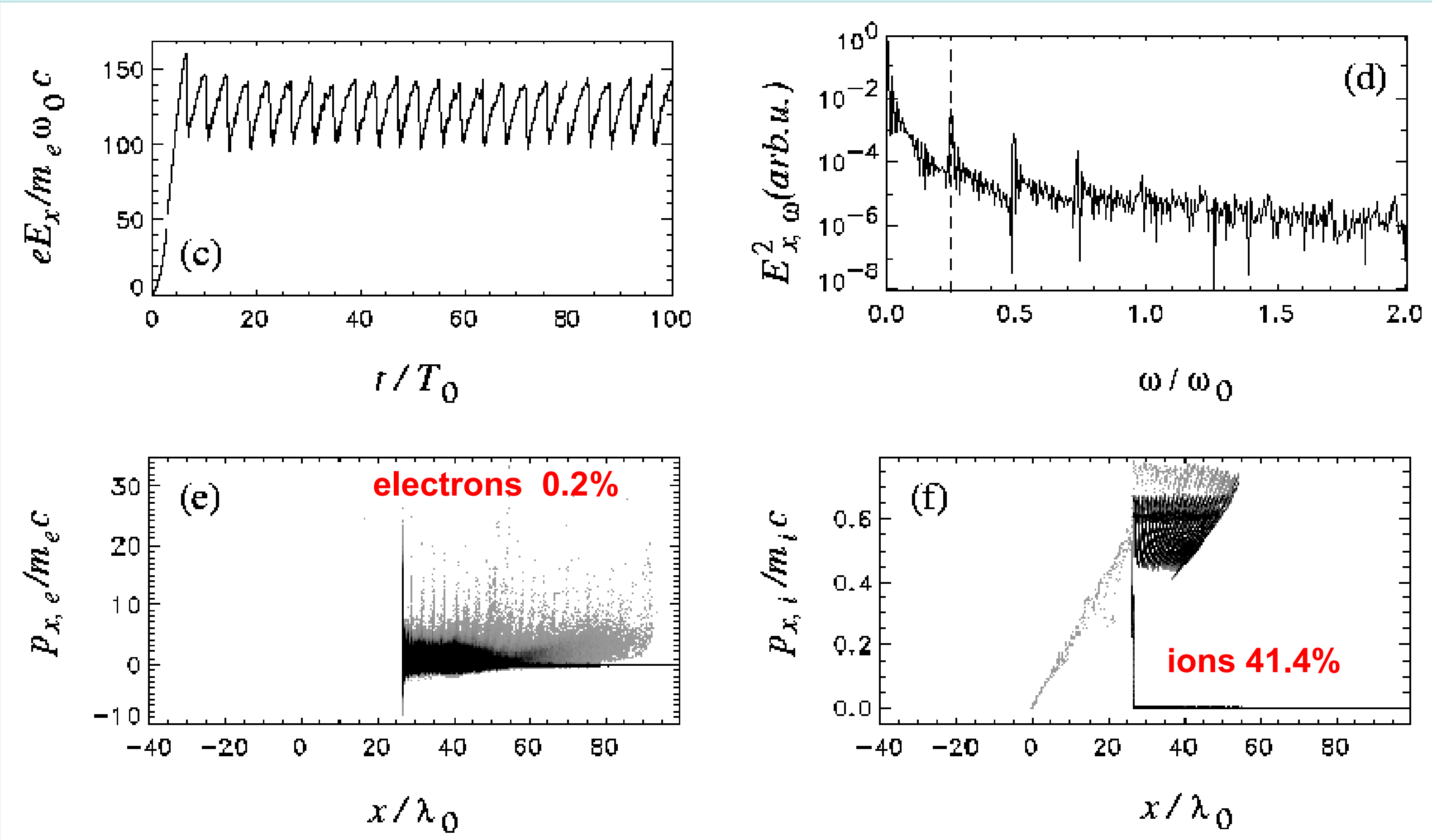

 Schlegel, Phys. Plasmas, 2009

Example of 1D PIC simulation: linear polarization

$a_0 = 20\sqrt{2}$, $I_0 = 1.6\times10^{21}$ W/cm^2 $n_0 = 20\ n_c$ $t = 100\ T_0$

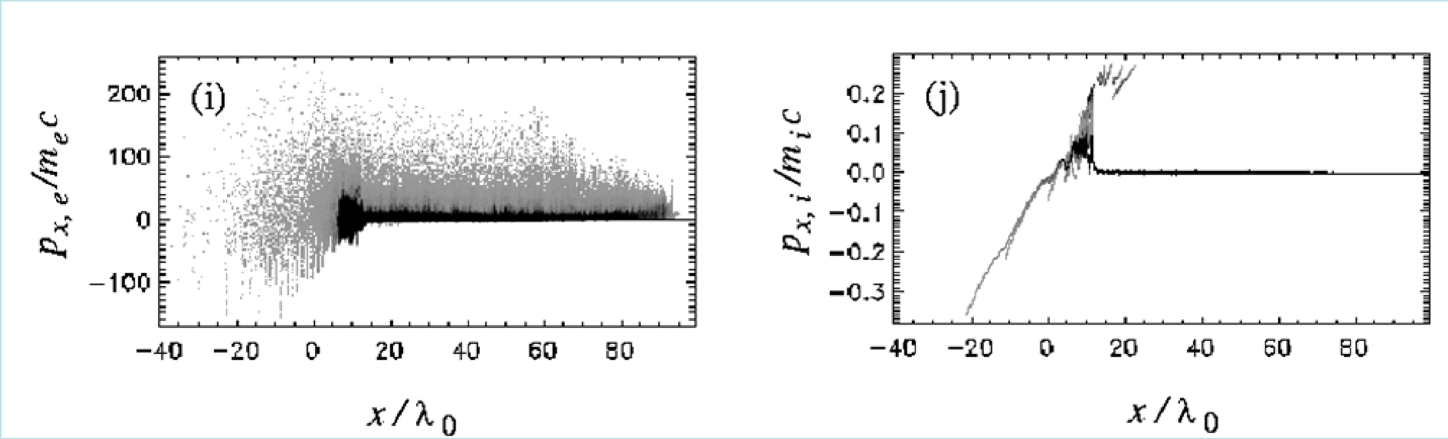

$a_0 = 100\sqrt{2}$, $I_0 = 4\times10^{22}$ W/cm^2 $n_0 = 20\ n_c$ $t = 100\ T_0$

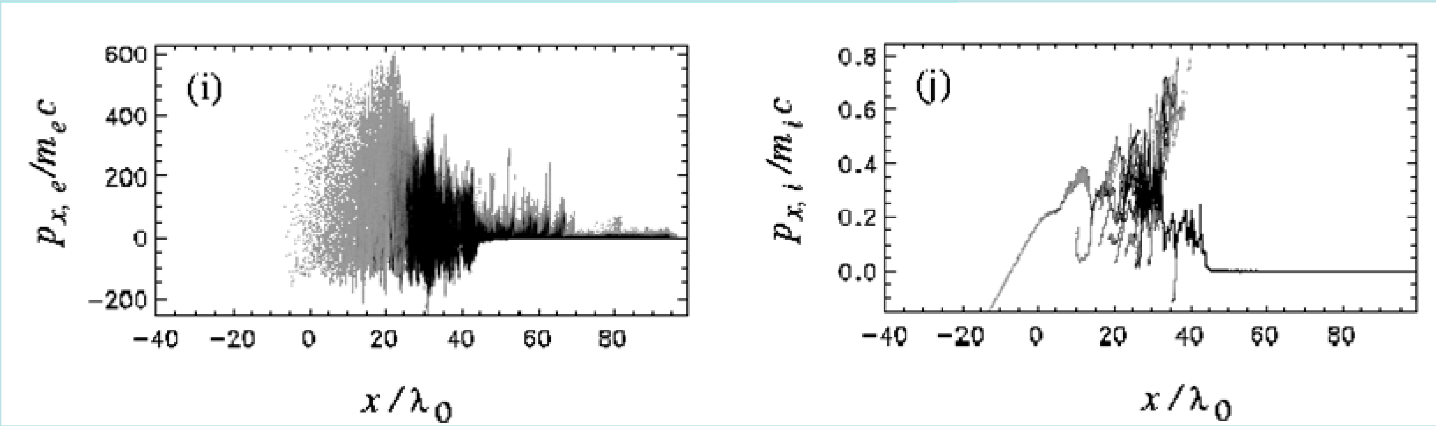

fast propagation of the laser light: induced transparency

Schlegel, Phys. Plasmas, 2009

1D PIC simulations with/without radiation reaction

a_0 = 100, circular polarization, $t = 100T_0$, plasma: $n_0 = 10n_c$, $m_i = 2m_p$

radiation losses : 43% | **without radiation losses**

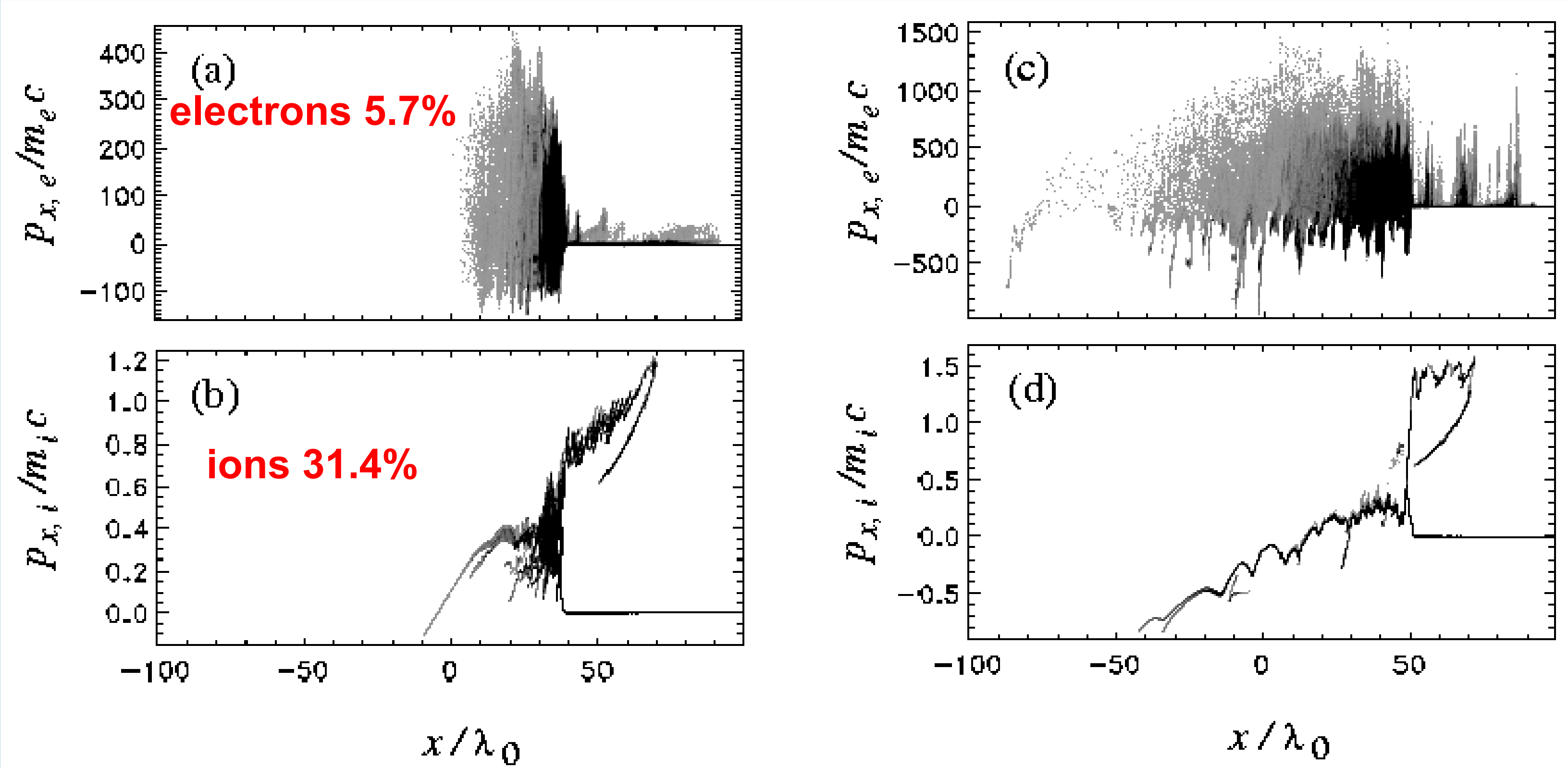

At low plasma density some electrons escape the ponderomotive potential if the ratio $a_0/(n_0/n_c)$ becomes too large. The radiation losses stabilize the piston

Schlegel, Phys. Plasmas, 2009

1D PIC simulations with/without radiation reaction

$a_0 = 100\sqrt{2}$, linear polarization, $t = 100T_0$, plasma: $n_0 = 10n_c$, $m_i = 2m_p$

radiation losses : 48;4%

without radiation losses

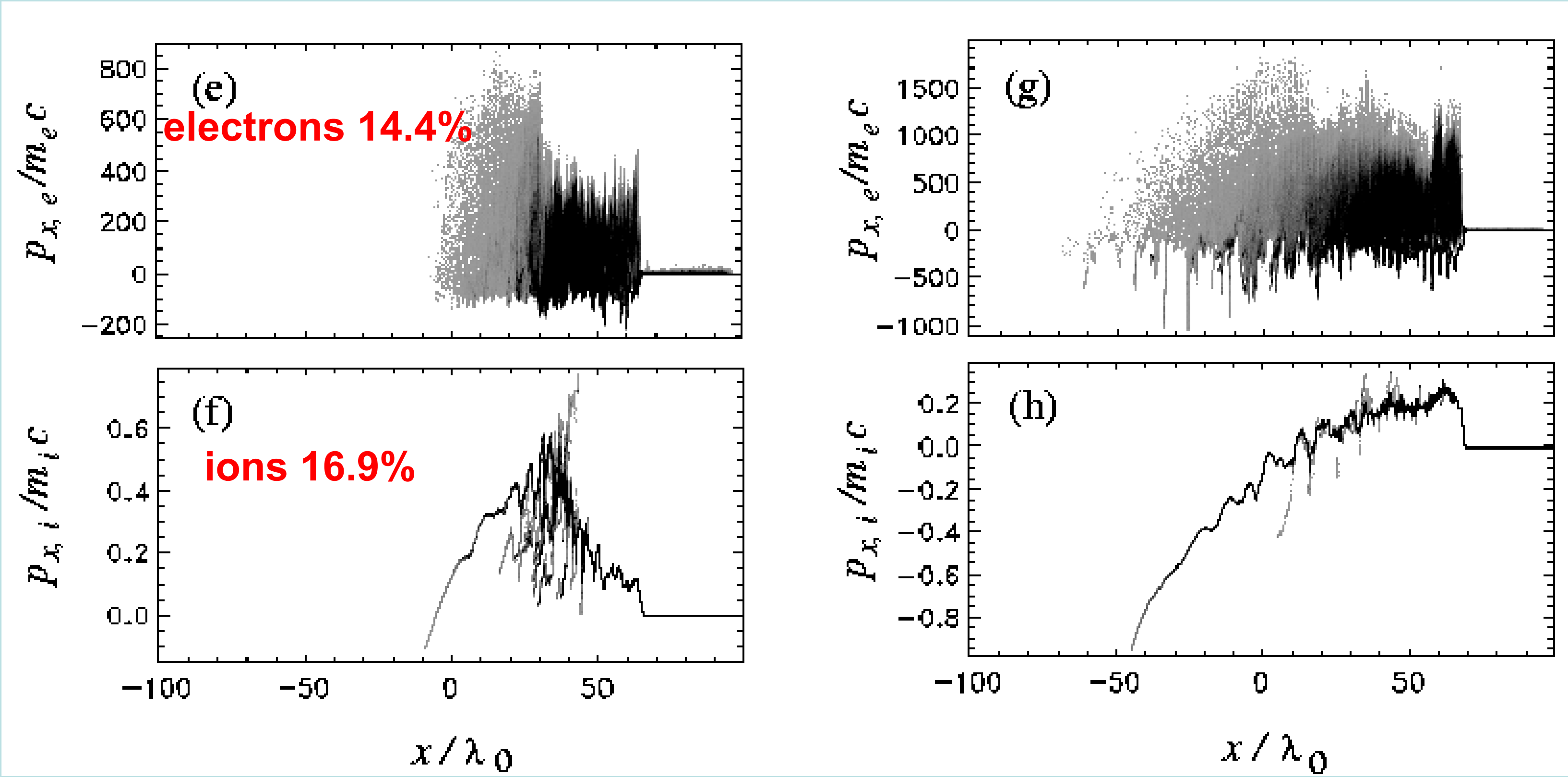

The radiation losses strongly depend on the laser intensity: for $a_0 = 20$ radiation losses are less than 1%

Schlegel, Phys. Plasmas, 2009

2D PIC simulation – channel formation

Flat-top laser intensity profile

- Ion density distribution demonstrates an efficient hole boring in the plasma, a clean and a stable channel
- Filamentation is strongly suppressed due to radiation pressure and radiation losses
- Velocity of hole boring is in agreement with the 1D model

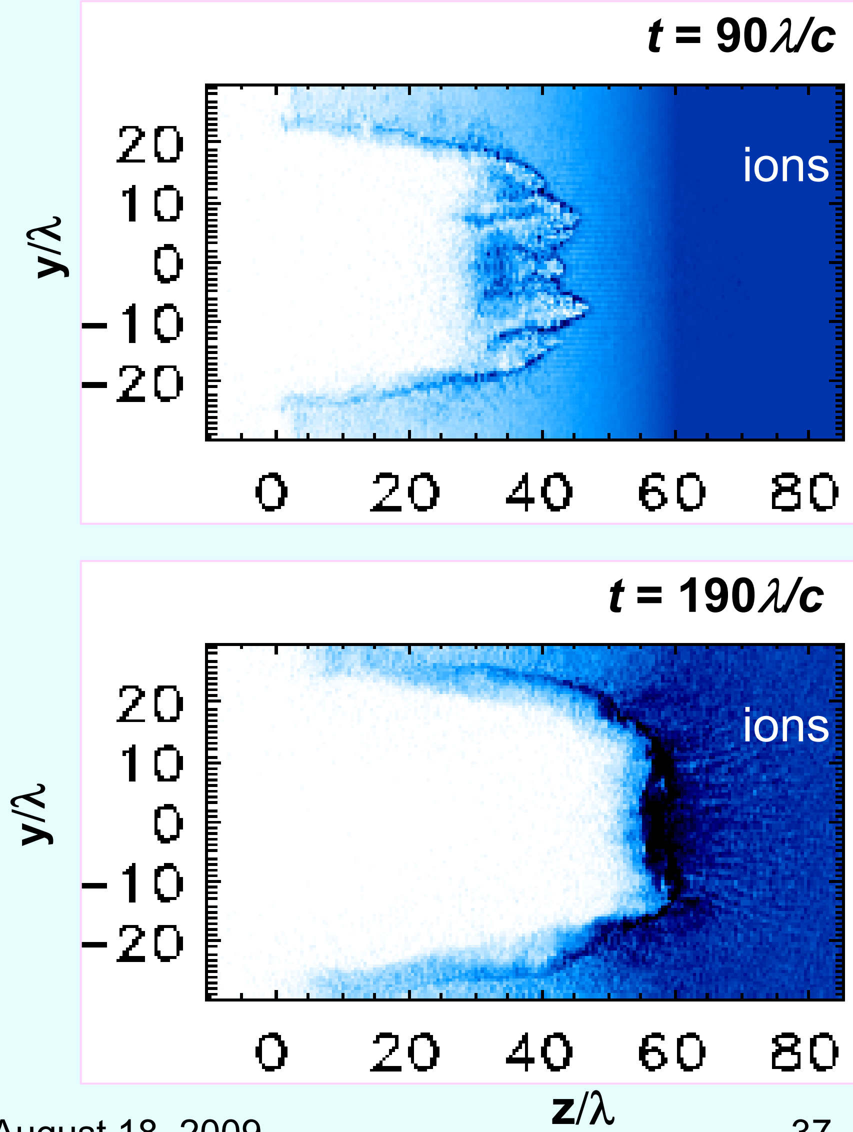

Naumova, Phys. Rev. Lett., 2009

2D PIC simulation – ion energy distribution and angular spread

- Angular distribution of ions *vs* energy at the final instant at $|y/\lambda| < 10$ shows a narrow peak in forward direction
- Energy distribution in the central part (a cone of 6^o) agrees well with 1D PIC simulations and analytical model

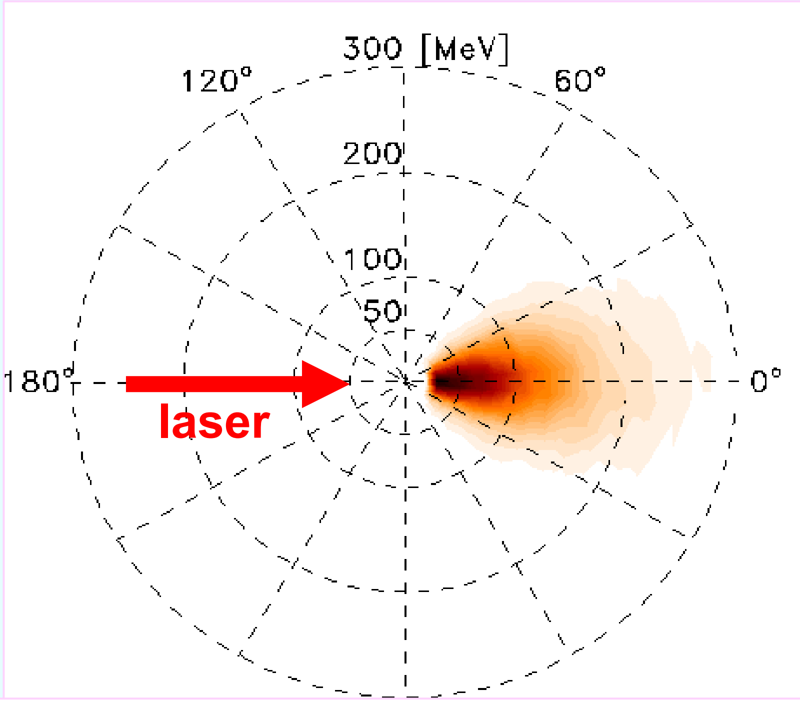

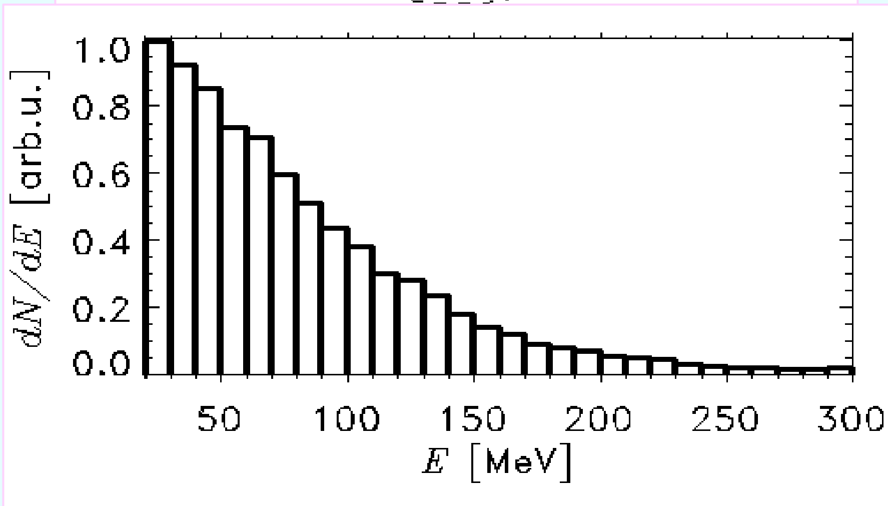

Naumova, Phys. Rev. Lett., 2009

Radiation acceleration of ultra-thin films

Light sail regime corresponds to acceleration of the whole foil under the laser radiation pressure;

The regime of acceleration change when the piston comes out of the rear side of the target $\tau_{las} > d/v_f$

Then the whole target is accelerated by the laser pressure:

very thin films and high laser intensities

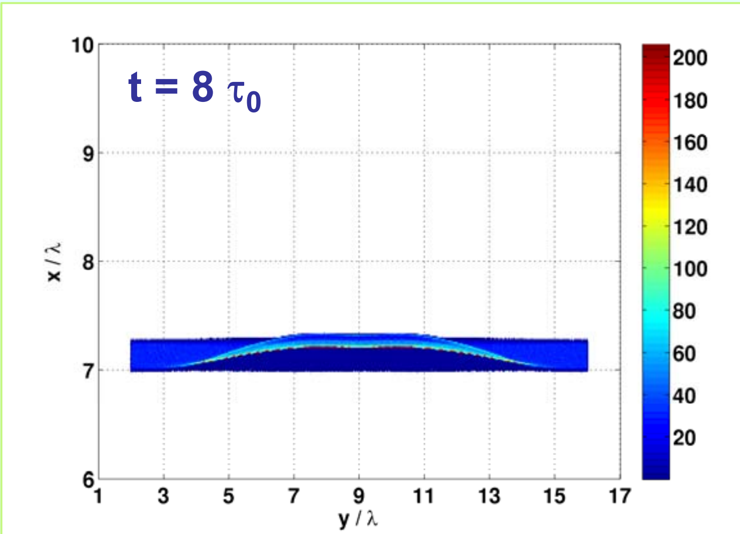

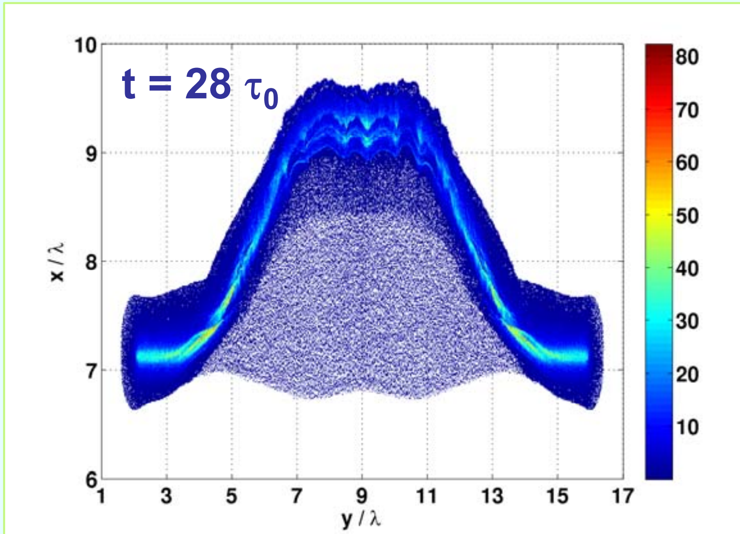

$I = 3\times10^{20}$ W/cm^2, $d = 200$ nm $\varepsilon_i \sim 150$ MeV

Klimo, PRST-AB, 2008

Model of the thin foil acceleration

Simple model considers a motion of the solid foil under the radiation pressure

$$n_e d \frac{\partial p_i}{\partial t} = 2R \frac{I_{\mathrm{las}}}{c} \frac{1-\beta_i}{1+\beta_i} \qquad \frac{\partial x_i}{\partial t} = \beta_i c$$

The minimum foil areal mass is defined by the reflectivity R (should be ≈ 1)

Linear case ($a_0 << 1$)

$$R = \frac{\varsigma^2}{1+\varsigma^2} \qquad \varsigma = \frac{n_e}{2n_c} k_0 d$$

Nonlinear case

$$R = 1 + \frac{1+\varsigma^2 - a_0^2}{2a_0^2} - \sqrt{\left(\frac{1+\varsigma^2 - a_0^2}{2a_0^2}\right)^2 + \frac{1}{a_0^2}}$$

Macchi, 2009, Vchivkov, Phys. Plasmas, 1998

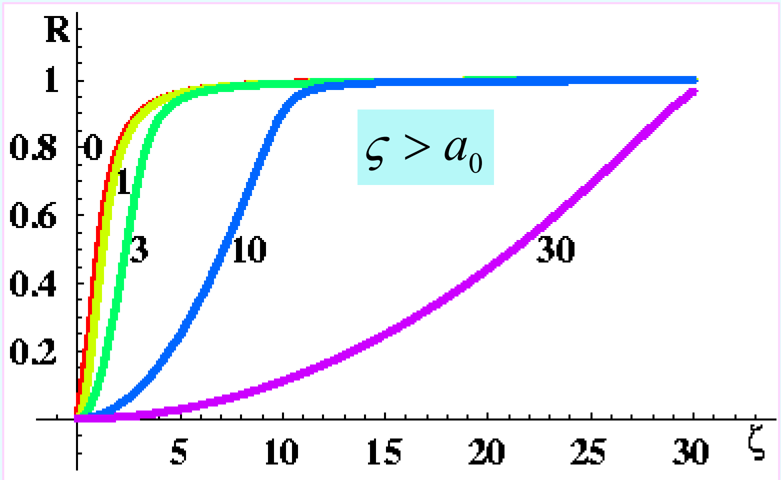

Reflectivity condition depends on the laser amplitude $e n_e d > 2\varepsilon_0 E_0$

Simulations of the thin foil acceleration

1D simulations show the details of ion acceleration: different ion species are accelerated to the same velocity

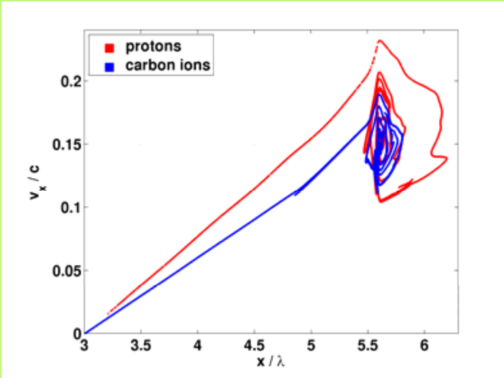

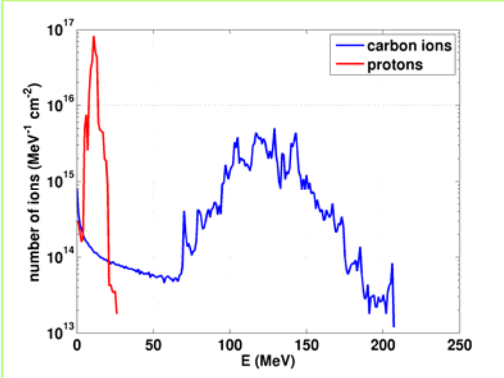

Intensity 3×10^{20} W/cm^2
Wavelength 800 nm
Duration 80 fs
Foil thickness 32 nm
Composition CH_2
Mass density 0.18 g/cc

2D simulations show the development of the foil instability and broadening of the energy distribution due to the Coulomb explosion

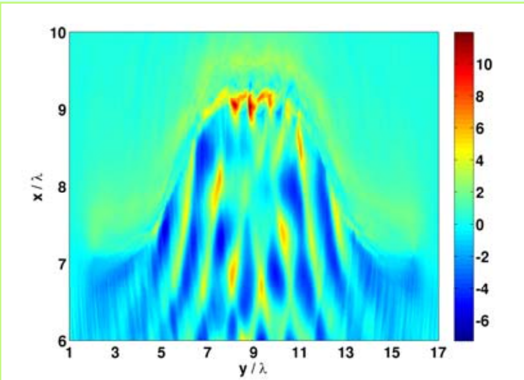

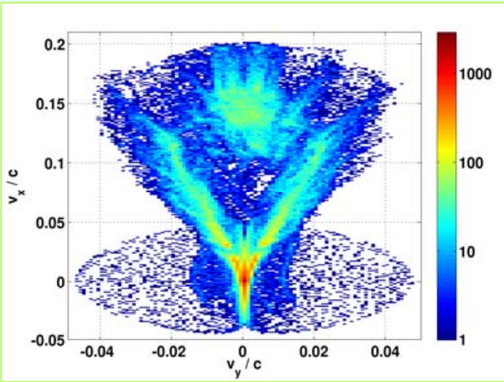

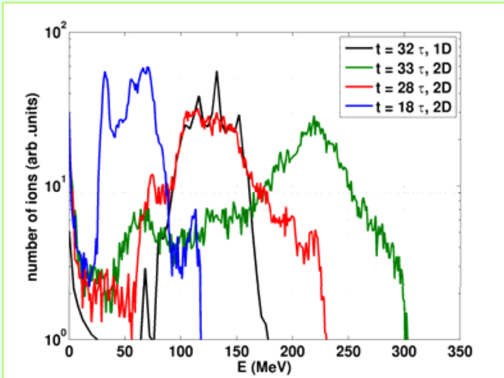

Klimo, PRST-AB, 2008

Applications of the laser accelerated ions

Specific features of laser accelerated ions:

- short acceleration length
- high charge
- good emittance

The energies of several hundred MeV will be probably achieved shortly with lasers pulses of a better quality (energy, duration, contrast)

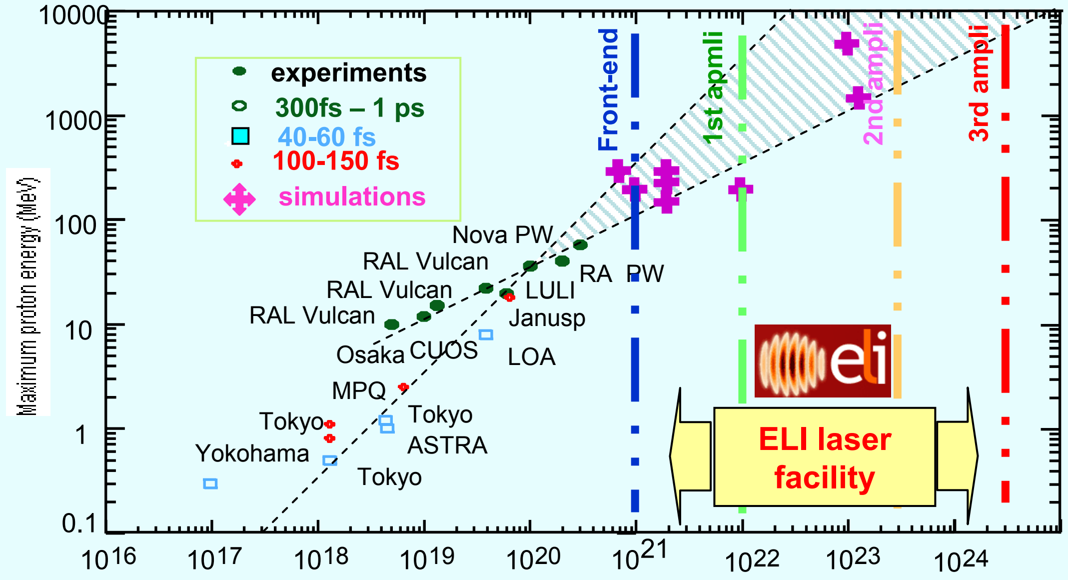

Fuchs, 2009

Analytical models and numerical simulations provide tools to control the ion beam characteristics, two competitive acceleration processes can be employed

Two European projects aim on the construction of lasers with enhanced capacities for the ion acceleration at extreme conditions (high intensities, ELI, and high energies, HiPER)

Smaller scale projects dedicated to the coordination of efforts on the national level for medical applications are under way in USA, UK, France, Japan, Germany

Radiography with fast ions

Laser accelerated ions are already demonstrated their potential for radiography of dense short-lived objects. They provide an access to high areal densities (> 1 g/cc), high temporal (< 1 ps) and spatial (< 1 µm) resolution of electric and magnetic fields

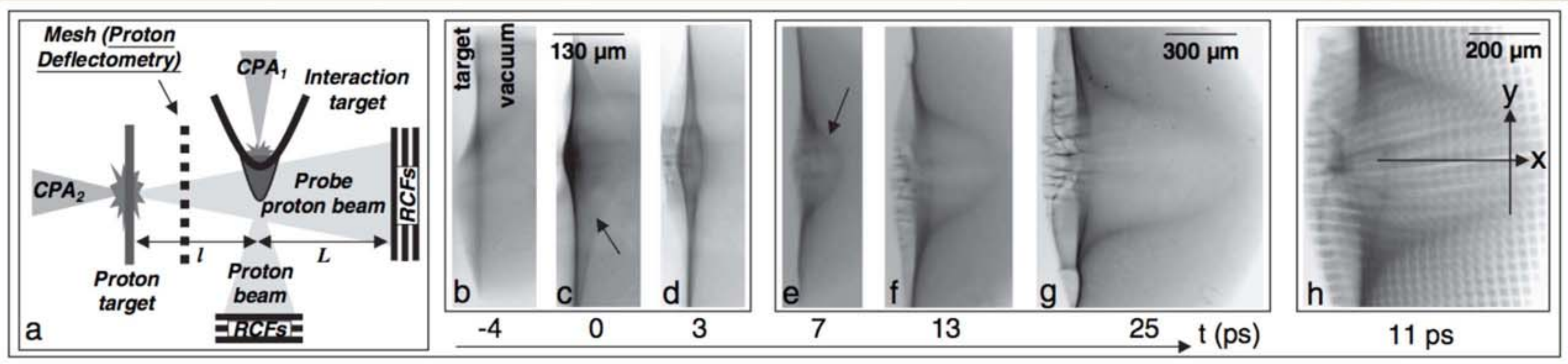

Romagnani, Phys. Rev. Lett. 2005

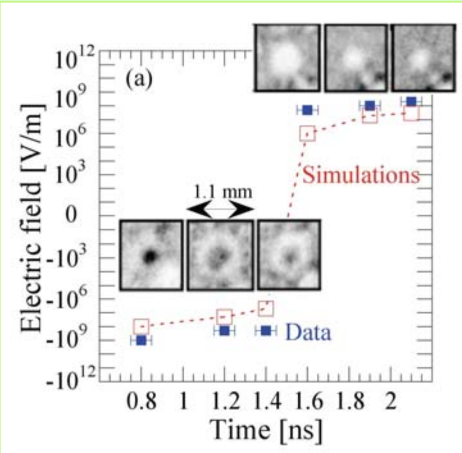

Li, Phys. Rev. Lett. 2005
Amendt, 2009

Extremely high electric fields up to 10^{10} V/m are measured

Medical applications

Laser produced ions are the attractive sources for the positron emission tomography. Production of the isotopes C^{11} O^{15} and F^{18} in pn reactions requires 20 – 30 MeV protons: 10 J, 1 Hz for production of samples with the activity of 200 – 300 MBq

For the cancer therapy the ions with energies of 250 – 350 MeV are required with a well controlled spectrum and high reproducibility

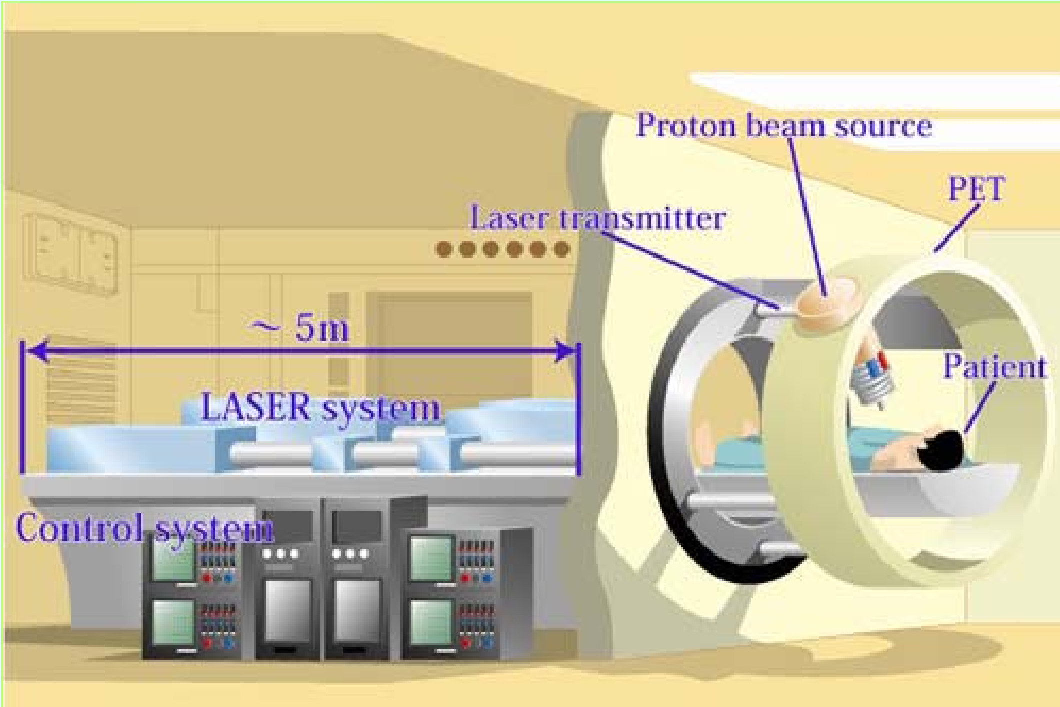

PMRC, Japan. 2009

Fast ignition with laser accelerated ions

Fusion target can be ignited with ions, they are more efficient than electrons because of a ballistic transport and a localized energy deposition.
Both acceleration methods are considered.
Required parameters: beam energy 10 kJ, beam radius at the deposition point 20 µm, pulse duration < 10 ps
Protons (deuterons) ion energy 10 – 20 MeV
Carbons: ion energy 400 – 500 MeV (30 – 40 MeV/n)

Indirect drive + TNSA ions

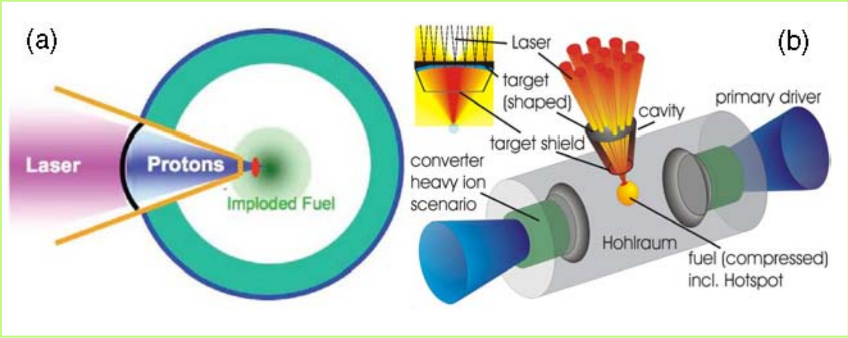

M.Roth, Phys. Rev. Lett. 2001

Direct drive fast ignition + RPA ions

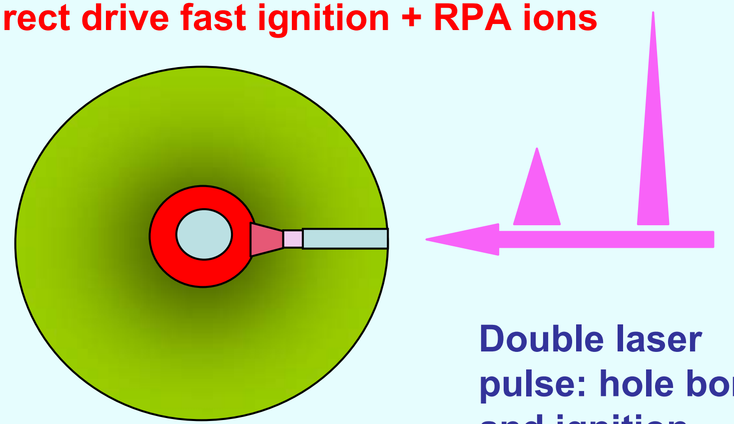

Double laser pulse: hole boring and ignition

temperature

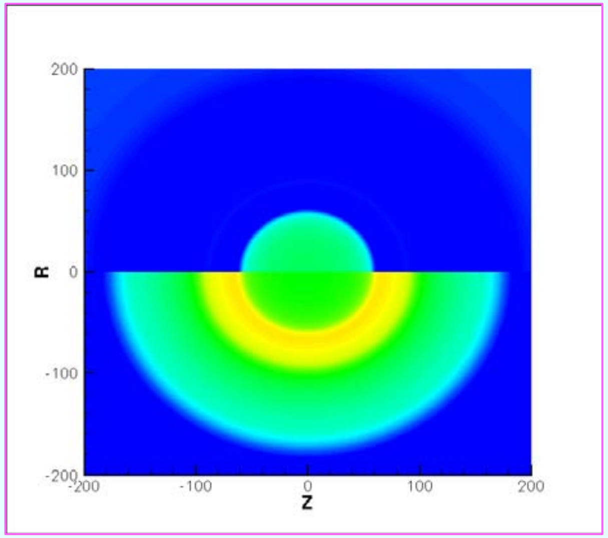

density

M.Temporal, 2009

The end

Many thanks to colleagues and co-authors who participated in these studies and in publications that are the base of this presentation

N. Naumova, ***Laboratoire d'Optique Appliquée, ENSTA, Palaiseau, France***
T. Schlegel, ***GSI, Darmstadt, Germany***
I. V. Sokolov, ***Space Physics Research Laboratory, University of Michigan, USA***
C. Labaune, ***Laboratoire d'Utilisation Lasers Iintenses, Ecole Polytechnique, France***
G. Mourou, ***Institut de la Lumière Extrême, France***
C. Regan, J.-L. Feugeas, Ph. Nicolaï, X. Ribeyre, G. Schurtz, ***Centre Lasers Intenses et Applications, Université Bordeaux 1, France***
M. Temporal, ***ETSIA, Universidad Politécnica, Madrid, Spain***
A.A.Andreev, Institute of Laser Physics, St. Petersburg
A.V.Brantov and V.Yu.Bychenkov, Lebedev Physics Institute, Moscow
***J. Limpouch, J. Psikal, O. Klimo*, Czech Technical University in Prague, Prague, Czech Republic**
***S. Ter-Avetisyan, M. Schnürer, T. Sokollik, P. V. Nickles*, Max-Born-Institut, Berlin, Germany**